Diplomarbeit

Giant cell tumor of bone (GCT)

Efficacy and safety of treatment with denosumab

eingereicht von

Lisa Jernej

zur Erlangung des akademischen Grades

Doktor(in) der gesamten Heilkunde

(Dr. med. univ.)

an der

Medizinischen Universität Graz

ausgeführt an der

Universitätsklinik für Orthopädie und Traumatologie

unter der Anleitung von

Sen.Scientist Priv.-Doz. Mag.rer.nat. Dr.scient.med.
Birgit Lohberger

Dr.med.univ. **Maria Anna Smolle**

Priv.-Doz. Dr.med.univ.et scient.med. **Iva Brcic**

Graz, 31.03.2021

Eidesstattliche Erklärung

Ich erkläre ehrenwörtlich, dass ich die vorliegende Arbeit selbstständig und ohne fremde Hilfe verfasst habe, andere als die angegebenen Quellen nicht verwendet habe und die den benutzten Quellen wörtlich oder inhaltlich entnommenen Stellen als solche kenntlich gemacht habe.

Graz, am 31.03.2021 *Lisa Jernej eh.*

Acknowledgements

With sincere gratitude, I would like to thank my three supervisors. This diploma thesis is a synopsis of very different departments of medical care as well as of basic research. Furthermore, I would like to thank *Medical University of Graz* for financial support by providing a scholarship.

First, I want to thank Priv.-Doz. Dr. Birgit Lohberger, for giving me the unique opportunity to work and learn in the orthopaedic laboratory at *University Hospital of Graz*. I got a peek in how basic researching functions and how important good cell culture practice and recording each step in an experiment is. At this point I would also like to thank MSc Dietmar Glänzer for being a good and patient teacher. My time in the lab was for sure characterized by ups and downs (side note: plastic chamber flasks do not work well with Xylol, as they just melt like plastic, so good that we never tried to make a HE chain from plastic chamber flasks using Xylol…), but as I see it, we never lost fun at our work and always found new solutions to bypass our previous problems. At least in the end, every experiment was successfully completed, as can be seen in the attachment.

Second, my great thank goes to Dr. Maria Anna Smolle. Thank you for always having an open ear to my problems, even if ambulance is overflowing with patients. Thanks for taking your time for meetings, even after a long night shift. The elective course “Papers, Posters and Presentations” arranged by you and the team of surgeons at the *Department of Orthopaedics and Trauma* is very helpful to learn the basics of scientific writing and statistical analysis. Overall, I want to thank the entire team for inspiring students to write abstracts, send them in for congresses and get a sneak peek into the scientific world without getting scared off.

Moreover, I would like to thank PD Dr. Iva Brcic for not only teaching me the histology of bone tumors, but also practically of every tissue that hit your table when I was there. You encouraged me, no matter how difficult project applications for biobank seem to a newcomer. The silence and peace in your office helped so much to work concentrated on the tumor data bank. And thanks for practically always giving me chocolate when I was at the *Department of Pathology*.

Contents

Abbreviations

ABC	Aneurysmal bone cyst
AP	Alkaline phosphatase
BFH	Benign fibrous histiocytoma
BMP	Bone morphogenic protein
CaSR	Calcium-sensing receptor
CDK4	Cyclin dependent kinase 4
C/EBPβ	CCAAT/enhancer binding protein β
CI	Confidence interval
COX 1	Cytochrome-c-oxigenase subunit 1
CT	Computed tomography scan
DAB	Diaminobenzidin-Tetrahydrochlorid
DCE-MRI	Dynamic contrast-enhanced MRI
DKK 1	Dickkopf 1
EDTA	Ethylenediaminetetraacetic acid
EMA	European Medicines Agency
FDA	United States Food and Drug Administration
FDG PET	Fluorodeoxyglucose-positron emission tomography
FFPE	Formalin-fixed, paraffin-embedded
FGFR-2	Fibroblast growth factor receptor 2
GCT	Giant cell tumor of bone
GPX1	Glutathione peroxidase 1
IHC	Immunohistochemistry

L2	2nd lumbar vertebra
LR	Local recurrence
MA	Mutational analysis
MAPK	Mitogen-activated protein kinase
MCP1	Monocyte chemoattraction protein 1
miRNAs	MicroRNAs, small ribonucleic acid fragments
MMP	Matrix metalloproteinase
MRI	Magnetic resonance imaging
mRNA	Messenger ribonucleic acid
NA	Not available
NFATc1	Nuclear factor of activated T cells c1
NGS	Next-generation sequencing
NOF	Non-ossifying fibroma
NOS	Not otherwise specified
OC-STAMP	Osteoclast stimulatory transmembrane protein
ONJ	Osteonecrosis of the jaw
OPG	Osteoprotegerin
PCR	Polymerase chain reaction
PDIA6	Member 6 of protein disulfide isomerase family A
PET	Positron emission tomography scan
PMMA	Polymethyl methacrylate (filling material)
PTHrP	Parathyroid hormone-related protein
RANK	Receptor activator of nuclear factor κB

RANKL	Receptor activator of nuclear factor κB – ligand
= ODF	Osteoclast differentiation factor
= OPGL	Osteoprotegerin ligand
= TNFSF11	Tumor necrosis factor ligand superfamily member 11
= TRANCE	TNF-related activation-induced cytokine
RUNX-2	Runt-related transcription factor 2
SATB2	Special AT-rich sequence-binding protein 2
SDF1	Stromal cell-derived factor 1
TACE	TNF-α-converting enzyme
TGF-β	Transforming growth factor-β
TNF	Tumor necrosis factor
TRAFs	TNF receptor-associated factors
TRAP	Tartrate-resistant acid phosphatase
VEGF	Vascular endothelial growth factor
WHO	World Health Organization

Glossary

H3.3/H3F3A	Gene where mutations of stromal cells are located
G34R/V/L/W	Mutations most important for pathophysiology of GCT
Neoplastic cells	Mononuclear stromal cells, harboring H3.3 mutations
Reactive cells	Macrophage-like cells and multinucleated osteoclast-like giant cells

List of Figures

List of Tables

Zusammenfassung

Einleitung

Riesenzelltumore des Knochens sind seltene intermediäre Tumore, die lokal destruktiv wachsen und in wenigen Fällen in die Lunge metastasieren. Betroffen sind meist junge PatientInnen zwischen 20 und 45 Jahren. Im Röntgenbild zeigen sich osteolytische Läsionen. Histologisch ist dies mit der Anwesenheit von osteoklastischen Riesenzellen mit bis zu 50 Zellkernen zu erklären, welche von den eigentlichen neoplastischen Tumorzellen rekrutiert werden. Der Therapieansatz der Wahl besteht in vielen Fällen aus einer rein chirurgischen Therapie, in herausfordernden Fällen allerdings steht auch eine systemische Therapie mit dem humanen Antikörper Denosumab zur Verfügung. Ziel dieser Diplomarbeit ist die Evaluierung der Effektivität und Sicherheit der Denosumab-Therapie.

Methodik

Die Durchsicht der orthopädisch-onkologischen Tumordatenbank diente der Analyse aller PatientInnen mit Riesenzelltumoren, welche seit 1998 an der *Universitätsklinik für Orthopädie und Traumatologie* therapiert wurden. Zur Diagnosesicherung erfolgte in Kooperation mit dem pathologischen Institut eine genaue histologische, immunhistochemische und genetische Aufarbeitung. Die statistische Auswertung erfolgte mit *IBM SPSS Statistics*, Version 26. Neun detaillierte Fallberichte über die Therapie mit Denosumab vervollständigten die Analyse.

Ergebnisse

Insgesamt wurden 54 PatientInnen analysiert, darunter 28 Frauen und 26 Männer. Das durchschnittliche Alter lag bei 37,9 Jahren. Hauptsymptom wie auch Hauptgrund, medizinische Hilfe in Anspruch zu nehmen, waren Schmerzen. Die Tumorgrößen schwankten zwischen 1 und 17 cm. Rezidive betrafen circa ein Viertel (25,9%) der PatientInnen. Alle PatientInnen erhielten primär eine chirurgische Therapie, in 9 Fällen wurde auch Denosumab zur Therapie verwendet. Im Mittel betrug der Beobachtungszeitraum 68,9 Monate.

Ein Fortschreiten der Tumorerkrankung unter Denosumab wurde in keinem Fall beobachtet. Kalzifizierung fand in 6 Fällen statt. In 6 Fällen wurde eine Operation durch Denosumab deutlich erleichtert, in einem weiteren wurde von einer chirurgischen Therapie gänzlich Abstand genommen. Symptomlinderung dagegen konnte in 3 Fällen nicht erzielt werden. Eine Nebenwirkung von Denosumab wurde beschrieben: An der Stelle der Injektionen trat eine kalzifizierte Weichteilläsion auf, welche chirurgisch entfernt wurde. Keine weiteren Nebenwirkungen traten auf.

Schlussfolgerung

Denosumab führte durch verbesserte Operationsmöglichkeiten zu mehr Beweglichkeit und besseren Therapieerfolgen. Radiologisches und histologisches Therapieansprechen war deutlich erkennbar. Schmerzreduktion konnte allerdings nicht immer erreicht werden. Hinsichtlich der Sicherheit von Denosumab traten keine Bedenken durch diese Analyse auf.

Abstract

Introduction

Giant cell tumors of bone (GCT) are considered as intermediate neoplasias due to locally aggressive growth and a rare tendency to metastasize. These rare lesions occur mostly in adults aged 20 to 45 years. Histological appearance is dominated by multinucleated osteoclast-like giant cells which are recruited by neoplastic cells and determine the osteolytic character of GCT. Treatment primarily constitutes of surgical therapy, however, systematic therapy with denosumab is recommended in calcitrant cases. This diploma thesis was set out to investigate efficacy and safety of denosumab, a human monoclonal antibody leading to formation of new bone.

Subjects

Fifty-four patients with GCT treated at the *Department of Orthopaedics and Trauma* between 1998 and 2020 were included into this retrospective analysis of tumor databank. Histological, immunohistochemical and mutational analyses took place in cooperation with the Institute of Pathology. Statistical analysis of all patients with verified diagnosis was performed using *IBM SPSS Statistics*, Version 26. Nine detailed case reports of every patient treated with denosumab concluded the analysis.

Results

Of all patients, 51.9% were female and 48.1% were male. Mean age at diagnosis was 37.9 years. Most common symptom as well as major reason for consultation was pain. Size of the tumors ranged from 1 up to 17 cm. Local recurrence affected approximately a quarter of all patients (25.9%). All patients received surgical therapy, 9 patients were also treated with denosumab. The mean follow-up was 68.9 months. Tumor progression under denosumab therapy was in no case observed, calcification took place in 6 patients. Denosumab improved surgical therapy in 6 cases and rendered amputation redundant in one young patient. On the contrary, reduction of pain could not be achieved in 3 cases. One adverse event was described: The patient developed a calcified soft tissue expansion where denosumab injections were administered. The lesion was surgically removed. No other side effects occurred.

Discussion

Therapy with denosumab facilitated better surgical therapy and led to increased mobility due to less invasive operations. Radiological and histological response was distinct. However, pain reduction could not be achieved in every case. Regarding safety of denosumab, no concerns derived from our analysis.

1 Introduction

According to WHO 2020 classification of soft tissue and bone tumors, osteoclastic giant cell-rich tumors are divided into 3 subgroups:
1) benign: aneurysmal bone cyst (ABC) and non-ossifying fibroma (NOF);
2) intermediate: giant cell tumor of bone (GCT) NOS;
3) malignant: GCT, malignant. (1)
This diploma thesis will focus on GCT NOS only.

Conventional giant cell tumors of bone (GCT) are characterized by locally aggressive growth and a rare tendency to metastasize. (2) Originally, GCT was considered an osteoclastic neoplasia and therefore named osteoclastoma. (3) However, fundamental new findings concerning functional biology resulted in acceptance that stromal cells are, in fact, the only neoplastic component of GCT. (2)

1.1 Epidemiology

Compromising 4% to 5% of primary bone tumors, GCTs are rare osteolytic lesions affecting mature bones occuring mostly in adults aged 20 to 45 years. Incidences among women are slightly higher than in men (with the exception of China, where a slight male predominance can be found). (4) Furthermore, it is hypothesized that GCT rates are higher in China than in the USA. (5) Emphasizing the rarity these lesions resemble, approximated incidences amount to 1.3 per million per year. (6, 7) Of note, less than 10% of GCT lesions are found in patients aged > 65 years. (8)

1.2 Pathophysiology

1.2.1 Cellular effects

Pathogenesis of GCT may be retraced by studying patterns of overexpression, or, on the contrary, suppression of various genes or proteins. Diverse mechanisms influencing tumorigenesis have been identified, thereunder modification of cell cycle as well as effects mediated by WNT/β-catenin and TGF-β (transforming growth factor-β). (9-11)

A connection between clonal aberrations affecting p53, GPX1 (glutathione peroxidase 1), MET and cyclin D1, and recurrence rates and malignant transformation of GCT can be found. (12, 13)

Altering the cell cycle of mononuclear cells, cyclin D1, cyclin B1 as well as Ki-67 play a major role in tumorigenesis. Overexpression of all three proteins is observed in mononuclear stromal cells, whereas in giant cells, only cyclin D1 is overexpressed. With respect to physiological functions, being regulation of G1 to S phase by cyclin D1 and regulation of S to M phase by cyclin B1, this seems to match evidence stating that multinucleated giant cells do not initiate M phase. (11)

Expression of cyclin D1 is up-regulated by c-JUN, which in return is related to various stress and growth factors and directly binds to CCND1 gene. Furthermore, cyclin D1 leads to tumorigenesis and cell proliferation by interaction with CDK4 (cyclin dependent kinase 4) and phosphorylation of pRB. Accumulation of cyclin D1 in nuclei is positively influenced by diverse protein expression, as well as activation of c-myc transcription, all together resulting in elevated cell proliferation. (14-16)

Glycogen synthetase kinase-3β is a major component of the WNT/β-catenin cascade and leads to degradation of both β-catenin and cyclin D1. Various influencing factors of glycogen synthetase kinase-3β exist, thereunder Ras, phosphatidylinositol-3-kinase and protein kinase B, resulting in activation of β-catenin and cyclin D1 through deregulation of glycogen synthetase kinase-3β. (10, 15) Furthermore, angiogenesis, differentiation of osteoclasts as well as tumor growth are induced by TGF-β mediated signals. (9)

1.2.2 Differentiation markers

Over the years, analysis of marker expression lead to further understanding of tumorigenesis, revealing an immature osteoblastic phenotype of neoplastic stromal cells characterized by expression of RUNX-2 (Runt-related transcription factor 2). The presence of RUNX-2 further initiates enzymes like alkaline phosphatase (AP), bone sialoprotein, type I collagen and osteopontin. Binding of RUNX-2 to core-binding factor α-1 is positively affected by BMP-2 (bone morphogenic protein) and BMP-6, two proteins also influencing osterix, another transcription factor of importance for tumorigenesis and cell differentiation. (17, 18)

Inactivation of pRB also plays a role in this process since phosphorylation of pRB (induced by cyclin D1) leads to invalidation of osteogenic mechanisms because RUNX-2 can also be stimulated by pRB (if not phosphorylated and hence inactivated). (19, 20) Another RUNX-2 downregulating factor is overexpression of TWIST, a major regulator of osteogenesis. (21) Suppression of FGFR-2 (fibroblast growth factor receptor 2) also contributes to interrupt osteoblastic differentiation. (22)

Osteoclast-like giant cells originate from osteoclast-precursor cells based on expression of differentiation markers and are recruited by mononuclear stromal cells which resemble the proliferating component of GCT. Neoplastic stromal cells not only express a surface marker of major importance, called RANK-L (receptor activator of nuclear factor κB – ligand), but also initiate osteoclastogenesis by secretion of cytokines and chemokines. The hereby resulting chemotaxis leads to recruitment of bone marrow-derived monocytes from the vascular system by MCP1 (monocyte chemoattraction protein 1) and SDF1 (stromal cell-derived factor 1). Recruitment of monocytes takes place by binding to CCR-2 and CXCR-4 (two cognate receptors). (17, 23) Along with activation of TGF-β by MMP-2 (matrix metalloproteinase) and MMP-6, these mechanisms are important processes leading to lysis of bone. (24)

1.2.3 RANK - RANKL interaction

RANKL (receptor activator of nuclear factor kappa B ligand) is expressed by neoplastic spindle-shaped mononuclear stromal cells, whereas RANK is located on the surface of multinucleated osteoclast-like giant cells. (25) Both RANK and RANKL belong to the TNF (tumor necrosis factor) family and play a major role in tumor associated lysis of bone. (26, 27) Located on chromosome 13 (13q14.11), the TNFSF11 gene encodes for RANKL, which can not only be found on neoplastic stromal cells of GCT lesions, but also physiologically on marrow stromal cells, monocytes, macrophages and pathologically in a variety of other tumors, including prostate cancer, breast cancer, chronic lymphocytic leukemia as well as primary multiple myeloma. RANKL itself has been renamed multiple times, considering synonyms like OPGL (osteoprotegerin ligand), TNFSF11 (tumor necrosis factor ligand superfamily member 11), ODF (osteoclast differentiation factor) and TRANCE (TNF-related activation-induced cytokine). (17, 28)

Developing from osteoclast precursor cells circulating in the blood stream, osteoclasts are recruited by neoplastic stromal cells via RANK - RANKL interaction. (23) Osteoclastic progenitor cells as well as osteoclasts are not only dependent of RANKL, but also induce cell death without stimulation trough RANKL. (29) Under physiological conditions, communication between osteoclasts and osteoblasts with regard to bone remodeling takes place via coupling factors produced from osteoclasts, leading to osteoblastic bone formation. (30) The opposite effect can be seen in GCT, where proliferating osteoclastic cells, recruited by RANK - RANKL interaction, seem to oppress mature differentiation of neoplastic cells to an osteogenic phenotype, determining osteolytic character of GCT lesions. (31) Denosumab, a human mononuclear antibody, inhibits interaction between RANK and RANKL, leading to suppression of function and maturation of osteoclasts and therefore initiates an osteoclast-depleted microenvironment. It is hypothesized that new formation of bone takes place through maturation of neoplastic stromal cells to a truly osteogenic phenotype in the absence of osteoclast expressed mediating factors, although still unknown. (32)

The RANK - RANKL interaction influences osteoclastogenesis and tumorigenesis through diverse pathways, including NF-κB mediated transcriptional alteration of κB-binding targets, MAPK (mitogen-activated protein kinase) regulated AP1 family members leading to expression of genes influencing malignant transformation, oncogenesis and osteoclastogenesis, and phosphatidylinositol signals, activating protein kinase C and Akt. Adapters regulating osteoclastogenesis are TNF receptor-associated factors (TRAFs) and Gab2. (13, 17, 28)

NFATc1 (nuclear factor of activated T cells c1) marks terminal differentiation of osteoclasts and is increased by RANKL-bound RANK, leading to up-regulation of multiple enzymes which in the end are responsible for osteolytic characters of GCT lesions. Bone resorption is essentially influenced by OC-STAMP (osteoclast stimulatory transmembrane protein), β3 integrin and cathepsin K. (17, 33, 34) Degradation of fibrillar collagen type I takes place by highly active cathepsin K, a papain-like cysteine protease. Dephosphorylation of bone sialoprotein and osteopontin facilitates migration of giant cells and is accomplished by TRAP (tartrate-resistant acid phosphatase).

Another factor found in multinucleated giant cells is αvβ3 integrin, enhancing movement of giant cells within bone matrix. (35, 36)

Several MMPs furthermore play a major role in metastasis, considering their effect on biological nature of GCT, enforcing aggressiveness through resorption of bone matrix. (24)

Expression of RANKL in GCT depends on many different factors. Using autocrine mechanisms, PTHrP (parathyroid hormone-related protein), influenced by CD40 ligand of T-lymphocytes, enforces RANKL expression on stromal cells. (37, 38) Decline of osteoprotegerin (OPG) and CaSR (calcium-sensing receptor) seems to be associated with an increase of RANKL expression, whereas the promoter of RANKL gains activity through direct binding of C/EBPβ (CCAAT/enhancer binding protein β). MMP-1 (matrix metalloproteinase -1) and TACE (TNF-α-converting enzyme) lead to release of soluble RANKLs from mononuclear stromal cells, enforcing osteoclastogenesis. (17, 39-41)

Interactions between neoplastic components of GCT (stromal cells) and reactive cells (recruited monocytes and osteoclast-like giant cells) are summarized in ***Figure 1***. (17)

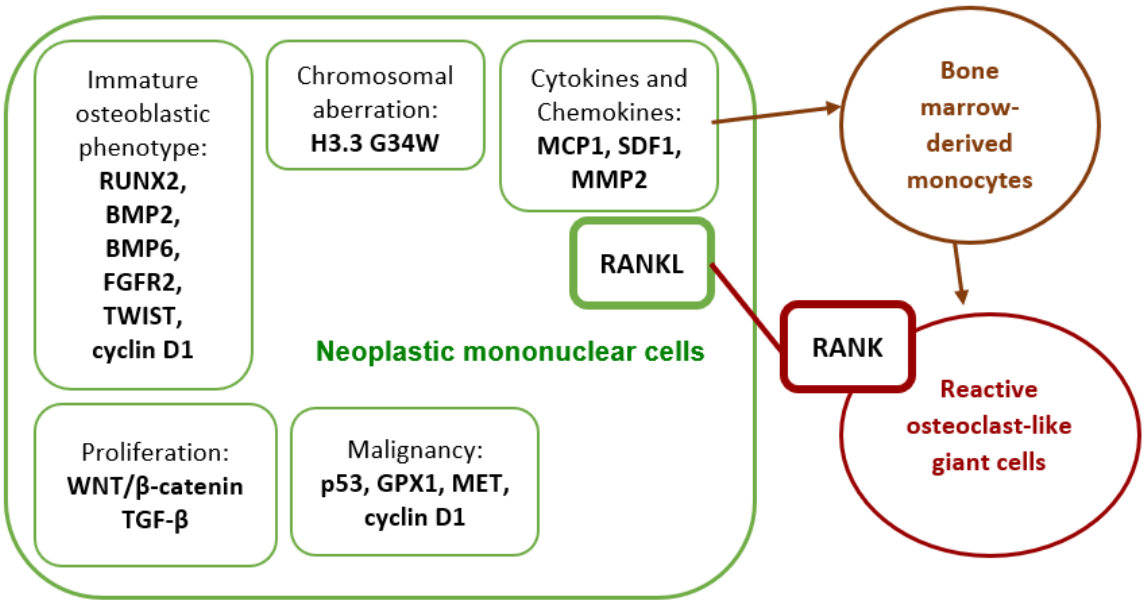

Figure 1

Summary of molecular pathways influencing tumorigenesis, depiction of relations between neoplastic stromal cells and reactive components of GCT. (17)

1.3 Molecular findings

In contrast to tumors affecting patients of higher age, pathologies among young adolescents or children show less intricated cytogenetic changes, resulting in easier identification of driving mutations. With respect to GCT, mutations in genes encoding histone H3 are characteristic, resulting in numerous modifications such as substitution of amino acids altering various post-translational modified amino acids. Substitutions associated with H3.3 gene mutations are named K36M, K27M and G34R/V/L/W, the latter being of great importance for tumorigenesis of GCT. (42, 43)

Mutations concerning histone H3.3 play a major role in identification of GCT. Two genes encoding H3.3 have been identified: H3F3A (chromosome 1) and H3F3B (chromosome 17). Mutations of H3.3 play a role in various tumors, including pediatric gliomas, chondroblastomas and GCTs. Mutations affecting these two

genes can help distinguishing lesions containing giant cells because H3F3 p.G34W mutation is characteristic for GCT, whereas H3F3B p.K36M mutation can frequently be found in chondroblastoma. (44)

Presence of H3F3A p.G34W mutation is reported in 85% to 95% of GCTs, other variants (G34L, G34M, G34R and G34V mutations) account for much smaller percentages of GCT lesions. (45-47) In fact, 92% of conventional, primary GCTs harbored G34W mutation, whereas in metastatic, recurrent, malignant or with denosumab treated GCT, G34W mutation was even found in all cases. Immunohistochemical staining using an antibody against G34W mutation is therefore of great importance in order to verify diagnosis. (48)

Of note, this antibody is specific for G34W mutation, in GCTs with other less frequent mutations, it shows negative reaction.

1.4 Histological findings

Histologically, GCTs are characterized by three different components: neoplastic stromal cells, macrophage-like round cells, and osteoclast-like giant cells (***Figure 2***). (2, 17) Intralesional hemorrhage often occurs. Lesions can vary in size, typically ranging from 5 to 15 cm. (2, 49)

The first component comprises of neoplastic stromal cells with spindle-shaped mononuclear fibroblast-like appearance and hardly defined cytoplasm. (17) Evidence suggesting that these stromal cells are in fact the only neoplastic cells derive from their dominance in the histological image, their higher proliferation rate, numerous genetic alterations and higher expression of important differentiation markers and cytokines. (50)

Beside these “neoplastic” cells, so called “reactive” cells are characteristic for GCT. Macrophage-like cells, resembling rounded mononuclear histiocytic osteoclast precursor cells, represent the second component. The presence of osteoclast-like giant cells with numerous vesicular nuclei and eosinophilic cytoplasm leads to the osteolytic character of GCT. These cells are recruited by neoplastic stromal cells and represent the third component. (4, 17)

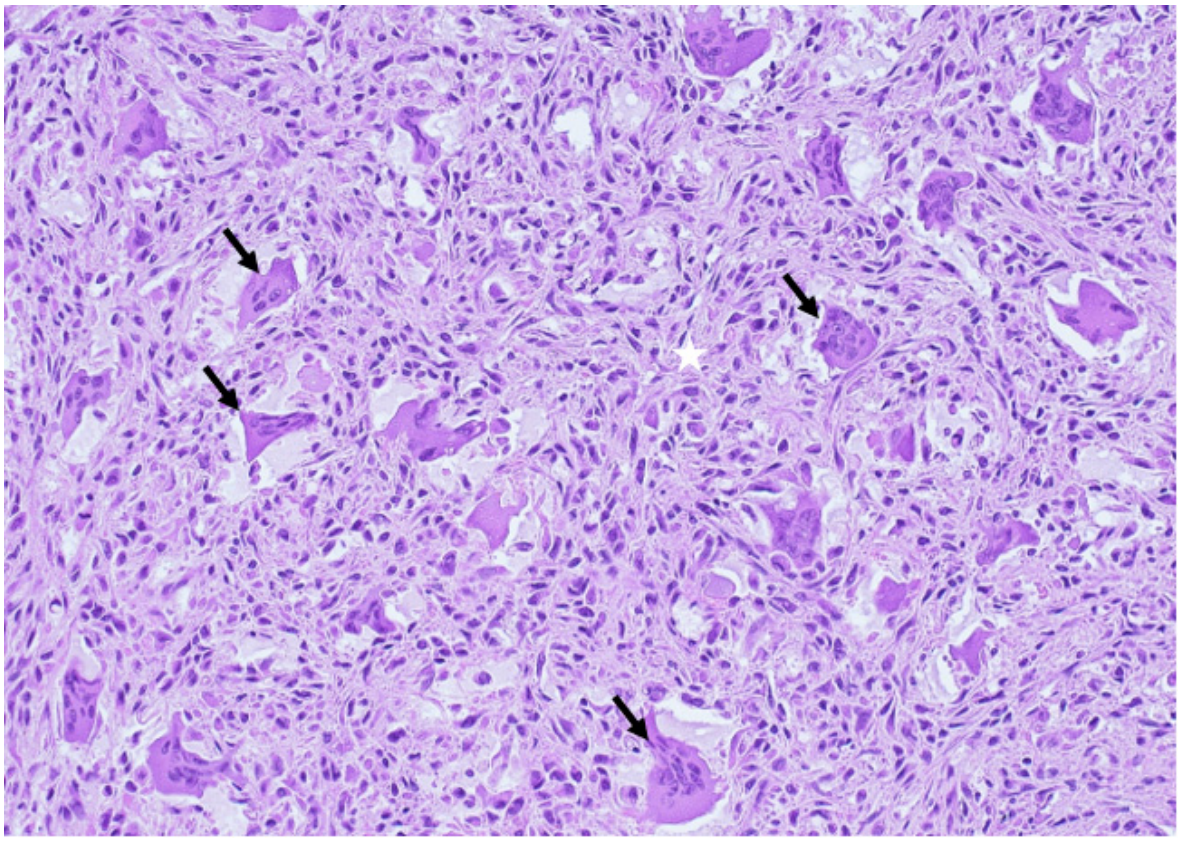

Figure 2

Histology of GCT: Reactive components of GCT lesions: rounded mononuclear histiocytic macrophage-like cells and multinucleated osteoclast-like giant cells (black arrows). Neoplastic spindle-shaped mononuclear stromal cells (white star). (Specimen from one of our GCT patients, HE staining, 20x magnification)

The number of nuclei in one giant cell can reach up to 50 and their similar appearance compared to the nuclei of neoplastic stromal cells helps distinguish diverse pathologies containing giant cells. Osteoclast-like giant cells can not only be found in benign or malign GCT, but also in a number of different lesions, including aneurysmal bone cyst, brown tumor arising in hyperparathyreoidism (also called Recklinghausen-disease), chondroblastoma, giant cell reparative granuloma, and giant cell-rich osteosarcoma. (2) However, differentiating these lesions containing giant cells can be accomplished by considering the differences in terms of radiologic aspects and other clinical features such as tumor location or age of patients. (17)

In addition, hemorrhage and siderophages as well as other secondary changes, namely secondary ABC (aneurysmal bone cyst) and necrosis, often occur. (49)

1.5 Immunohistochemistry

With respect to cases where pathologists cannot for sure identify GCT lesions, immunohistochemistry may help distinguishing GCTs from a variety of other pathologies. (17)

Analysis of mutations existing in GCT through immunohistochemical staining showed that the majority of mononuclear cells that can be found in GCT harbor G34W mutations, resembling neoplastic stromal cells. Mononuclear cells negative for G34W mutation are thought to be histiocytic components. However, G34W mutation has not been found in nuclei of osteoclast-like multinucleated giant cells, which can be considered as further evidence indicating a reactive, non-neoplastic nature of giant cells. Equally non-positive for this mutation were other components forming GCT lesions, such as lymphocytes, foamy histiocytes, vascular smooth muscle cells, endothelial cells and fibroblasts. G34W mutations are also harbored in lesions associated with GCT, especially in secondary aneurysmal bone cysts. Evidence suggesting that decalcification as well as degenerative changes decrease sensitivity of sequencing using Sanger methods (due to increase of non-neoplastic cells) leads to the presumption that immunohistochemistry might even be more cost-effective and sensitive than PCR. (48)

1.6 Differential diagnoses

Benign fibrous histiocytoma (BFH) and non-ossifying fibroma (NOF) are important differential diagnoses considering that most GCTs show areas similar to the histological appearance of BFH and NOF. Chondroblastoma are common in skeletally immature patients. Further, the nuclei of mononuclear stroma cells do not resemble nuclei of osteoclast-like giant cells. The same can be said about giant cell reparative granuloma, also called brown tumor. Distinction between primary aneurysmal bone cyst (ABC) and cystic GCT is especially calcitrant. For diagnosis of GCT with secondary ABC, typical morphology of GCT must be evident. Giant cell-rich osteosarcoma comprises another differential diagnosis of GCT. (49)

1.7 Clinical findings

The conventional type as well as the malignant type of GCT arise in similar localizations. (51-53) GCT lesions most commonly occur in mature skeleton at the meta-epiphyseal region, typically affecting the distal femur, proximal tibia, proximal humerus and distal radius. Development in the immature skeleton is less frequent. (52) If the axial skeleton is involved, the vertebral body and sacrum are the most common localizations. (54, 55) The pelvis is the most frequently involved flat bone. Nevertheless, appearance in flat bones is uncommon, similar to tubular bones. (46, 56) Another rare localization are the gnathic bones. (46, 57) Of note, GCT can also occur multicentric. (2) ***Figure 3*** shows locally destructive growth of a lesion, which is common for GCT.

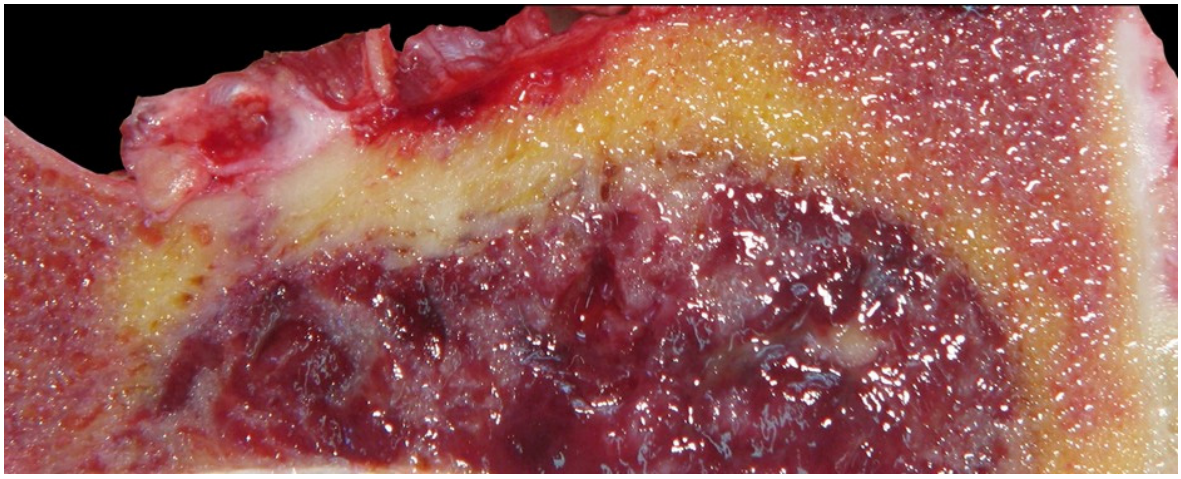

Figure 3 *GCT of one of our patients, located at the superior pubic ramus.*

A typical clinical sign of GCT is pain, either at night while resting, as tumor growth leads to expansion of periosteum, or upon weight bearing, caused by loss of mechanical stability of affected bones. Patients' history often comprises a 3-6 month period of pain, followed by wrong initial diagnoses like intraarticular derangement or arthritis. Findings of physical examination may include tenderness to palpation, swelling of soft tissue, direct or sympathetic joint effusion and gaits favoring the affected side in order to achieve an antalgic effect. Pathological fractures due to bone resorption are most often observed in the distal femur, in general occuring in 5-12% of patients. (2, 58-60) Fracture lines can also affect the adjacent joints and therefore may complicate surgical therapy of GCT. However, local recurrence and metastatic rates are not affected by fractures. (2)

Table 1 shows the two different staging systems that exist regarding GCT. First, Enneking Staging can be used, which grades lesions by biological nature and growth. Second, Campanacci Grading System divides lesions in three categories, taking imaging analyses into account. Stage or grade 1 of both systems is a rarity among GCT lesions, seeing as most lesions are grade 2 or stage 2. In advanced GCT, soft-tissue masses can arise to huge extent, even affection of neighbouring bones is possible when tumor growth crosses ligaments. (2) However, these systems are not clinically relevant. (4)

STAGE / GRADE	*ENNEKING STAGING SYSTEM*	*CAMPANACCI GRADING SYSTEM*
1	Biologically stable, benign, indolent	Radiologically no signs of aggressive growth, well-circumscribed lesion
2	Progressive growth within natural barriers	No radiopaque rim in relatively well- defined borders
3	Aggressive growth, soft-tissue mass	Cortical bone destruction, soft tissue mass, ill-defined borders

Table 1

Enneking Staging System and Campanacci Grading System of giant cell tumors of bone. (2)

GCT recurrence rates are quite high, with 15-50% of conventional GCT lesions showing local recurrence, most commonly within 2 years after surgery. Metastases in the lung can be found in 3-7% of patients. (4)

Pulmonal metastases presumably are lesions resulting from embolization of intravascular growing GCT and show only slow progression, in some cases even disappearing sponateously. However, death due to respiratory failure is reported in rare cases. (61, 62)

1.8 Radiological findings

The first step in diagnosing primary or recurrent GCT consists of a conventional X-ray radiograph, where lesions typically arise in the metaphysis of long bones, further reaching to the epiphysis and subarticular region. Eccentric location and lytic character with sharply defined and non-sclerotic borders are typical features of GCT, as ***Figure 4*** shows. Fine to coarse trabeculation is also common, representing endosteal ridging. Soft tissue components as well as cortical destruction can be seen in more aggressive lesions. Computed tomography (CT) provides a more detailed view regarding pathological fractures, fracture lines and cortical thinning and therefore might be necessary before performing intralesional surgery. (63, 64) Prediction of clinical behaviour and staging requires a Magnetic Resonance Imaging (MRI), commonly showing low to intermediate signal intensity on T1-weighted images and intermediate to high intensity on T2-weighted images. Furthermore, extension of GCT lesions not only within the bone, but also within soft tissue components can be assessed through MRI and is of great importance for planning of surgical therapy. Particularly on gradient-echo sequences, haemosiderin deposits lead to low signal intensity. Secondary aneurysmal bone cyst-like alterations result in fluid-fluid levels and can be seen in 10-14% of GCTs. (63-65) Rapidly progressive and early enhancement as well as quick wash out of intravenous applied gadolinium can be seen when using dynamic contrast-enhanced MRI (DCE-MRI). (66)

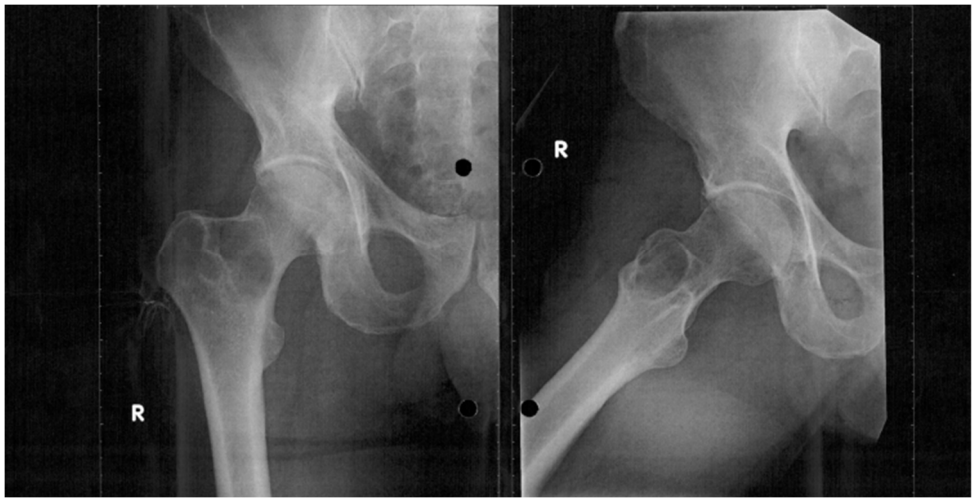

Figure 4

GCT located at the proximal femur. (Radiography of one of our GCT patients.)

1.9 Therapy

1.9.1 Surgical treatment

Therapeutic options of GCT generally depend on localization of lesions, considering that GCT of bones regarding the appendicular skeleton are commonly best treated with curettage plus local adjuvants or en-bloc resection, whereas surgical therapy of lesions in the sacrum and axial skeleton often is associated with complications due to proximity to delicate neurovascular structures and complex anatomy. (67) Timing of surgery should individually be evaluated. Waiting for healing of extra-articular fracture lines may be appropriate, whereas immediate surgery should be favored in case of dislocation or intraarticular fractures with incongruent joints. (68)

Mainstay of therapy in primary GCT lesions is intralesional curettage. Considering the high recurrence rates in lesions treated with surgery alone, however, local adjuvants play an important role in surgical treatment. Adjuvants decreasing risk of local recurrence to 17% are bone cement, liquid nitrogen, hydrogen peroxide and phenol. These chemicals are more effective than the use of sterile water alone. Use of ethanol or phenol leads to same effects on local recurrence rates but ethanol proofs superior considering safer and easier application. Therapy including coagulation through an argon beam laser is useful in terms of extended reach in which curettage declines cellular tissue. (69-71) A mechanical adjuvant is high-speed burring. (72) Packing of defects left after curettage takes place using allografts or polymethyl methacrylate (PMMA) cement. (2, 73)

Further decrease of local recurrence rates down to <8% can be accomplished by cryosurgery. Hereby liquid nitrogen gets directly applicated into the tumor cavity, serving as a freeze-thaw couplet extending depth of curettage by destroying cells located further away from burred surface. Of note, treatment with cryosurgery is especially controversial due to high risk of complications such as vascular injuries and pathological fractures, but improvement of technical methods including prophylactic osteosynthesis and precise observation of freezing temperature have led to a distinctive decrease in rates of pathological fractures. Where in the past fractures occurred in 25-50% of cases, only 0-7% are seen with advanced techniques lead. (74-77) En-bloc resection of GCT lesions followed by

reconstruction with either endoprosthetic implants, structural or bulk allografts is associated with higher complication rate and morbidity, including allograft failure, aseptic loosening of endoprosthetic replacement and non-union. This therapeutic option is therefore considered appropriate only for challenging GCT lesions where systemic treatment as well as intralesional curettage are impossible, as shows ***Figure 5***. Indications for en-bloc resection are cases such as tumors including wide masses of soft tissue components neighboring neurovascular structures, curettage with poor functional outcome due to impossible joint reconstruction, acute compression of myeloma, intra-articular fractures associated with immediate indication for surgery as well as lesions localized in so called expandable bones like proximal and mid fibula, distal ulna and clavicle. Complications of curettage including use of adjuvants occur most often when cryosurgery or bone grafting is performed. Besides pathological fractures, infection, transient or permanent nerve paralysis, non-union and secondary osteoarthritis can occur. (2, 67, 74, 78)

A new possible treatment option is substitution of PMMA with similar agents leading to same oncological outcomes but less risk of secondary osteoarthritis. (79-81)

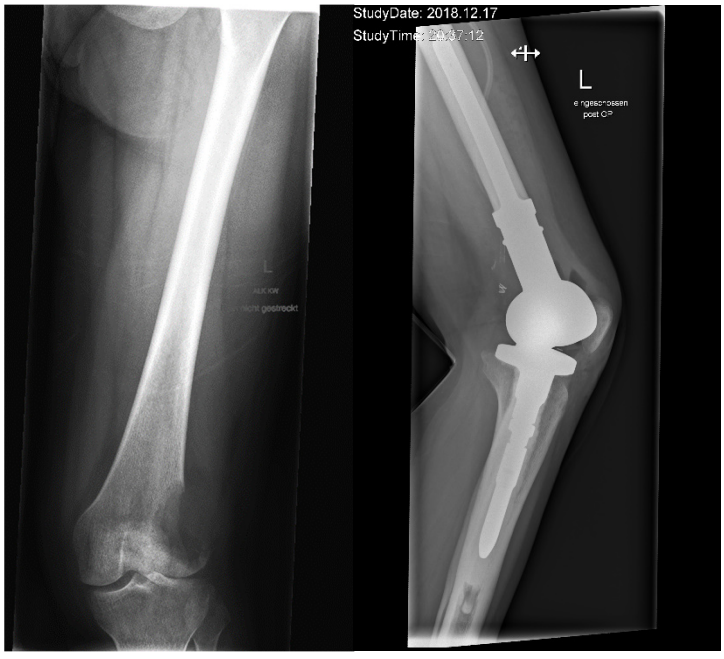

Figure 5 *Left side: Osteolytic GCT lesion located at the distal left femur. Right side: Implanted endoprosthesis. (Radiography of one of our GCT patients.)*

1.9.2 Radiotherapy

Radiotherapy plays only a minor role in new multidisciplinary treatment regimens of GCT and is restricted for seldom and difficult cases in which lesions appear unresectable, recurrent or residual and therapy with denosumab is impossible, due to contraindications, ineffectiveness or unavailability. In these selected cases, radiotherapy can be seen as an option with acceptable oncologic outcome, with local control rates of approximately 80%. (82) Disadvantages of radiotherapy are intra- and postoperative complications in case surgery is required, as well as a lifelong increased risk of radiation-induced sarcoma, developing in 3-11% of patients. (83, 84) Among different radiotherapeutic methods, photon therapy is considered problematic when applied at locations near the spine, considering possible side effects damaging the spinal cord. Carbon ion or proton radiotherapy may be more advantageous in these locations. (67)

1.9.3 Bisphosphonates

Efficacy of therapy with bisphosphonates is not well evidence based. However, this treatment option is thought to have a more direct effect on GCT than denosumab due to direct inhibition of mRNA expression of RANKL in neoplastic stromal cells. It is proposed that through application of zoledronic acid, binding to bone mineral takes place, thus leading to suppression of osteoclast formation and migration, inhibition of osteolysis and bone resorption, and furthermore inducement of cell death among osteoclasts. (85)

However, after a few months of bisphosphonate therapy, not only inhibition of bone resorption can be seen, but also a halt in bone production. The mechanisms behind this finding are still largely unknown, although communicational signaling between osteoclasts and osteoblasts presumably play an important role. Bisphosphonates and denosumab both seem to affect the Wnt/β-catenin pathway, considering alterations of serum concentrations of two factors named sclerostin and DKK 1 (Dickkopf-1) that inhibit signaling of Wnt pathways through binding to Wnt co-receptors. (86-88) Evidence regarding treatment of postmenopausal osteoporosis with denosumab proofs an increase of sclerostin and a decrease of DKK 1 in serum due to denosumab. In contrast to therapy with denosumab, use of bisphosphonates does not result in a decrease of DKK 1. This might be attributable to a difference in therapeutic mechanisms of these two drugs.

DKK 1 is physiologically expressed in osteoblasts and maturing osteocytes. Bisphosphonates mostly target mature osteoclasts, leading to an increase of osteoclast precursors, whereas denosumab inhibits recruitment of osteoclast precursor cells. (88-90) Long time treatment with bisphosphonates does lead to an increase of concentration of sclerostin in the serum, enforcing the presumption that decrease of new bone formation after a longer period of zoledronic acid application may be associated with an increase of sclerostin. Decrease of DKK 1 due to denosumab treatment might reduce decrease of bone formation mediated by increase of sclerostin. (88, 91)

Bisphosphonates can either be used in a neoadjuvant treatment setting or as a local adjuvant together with PMMA or artificial bone after curettage. However, further evaluation of oncological outcomes after use of zoledronic acid is necessary. (92, 93) Osteonecrosis of the jaw (ONJ) is a severe complication both of bisphosphonate and denosumab therapy. (94, 95)

1.9.4 Denosumab

In 2013, denosumab was registered by the United States Food and Drug Administration (FDA), administration by the European Medicines Agency (EMA) followed 2014. (96) Beside unresectable GCT or cases of GCT where planned surgical treatment would be associated with presumably high morbidity, other indications for the use of denosumab are osteoporosis, hypercalcaemia of malignancy or bone metastases resulting from solid tumors. This drug mediates through inhibition of interaction between RANK (receptor activator of nuclear factor kappa B) and RANKL (-ligand). By binding to RANKL with high specificity, this fully human monoclonal antibody therefore imitates osteoprotegerin. (97) Blocking the recruitment of osteoclast-like giant cells by RANK-positive mononuclear macrophages or preosteoclasts leads to suppression of bone resorption. (25, 98, 99)

Denosumab plays a major role in advanced GCT. Invasive operations such as amputations or en-bloc resection can be prevented through systemic use of this drug in a multidisciplinary treatment. The goal of this therapy is not only to achieve local control and stop tumor growth in order to minimize morbidity of following surgical treatment, but also render operations completely redundant. (99, 100)

Patients undergoing denosumab therapy showed after an average time of 3-4 months shrinking in tumor size as well as calcification of the rim surrounding the tumor and soft tissue. Further spreading of calcification can be seen depending on therapy duration. Calcifying processes enclosing the whole tumor also contribute to reduction of therapy morbidity because curettage can easier be accomplished this way. (99-101) Especially considering advanced GCT of the axial skeleton, where in the past location and size of the tumor might have made surgery impossible, neoadjuvant use of denosumab facilitates new treatment perspectives. (102)

Therapy with denosumab provides clinical benefits for patients, considering pain relieve as well as more mobility and better function achieved through less invasive surgically treatment. Concerning the influence of denosumab on local recurrence rates, inconsistent conclusions can be found in literature. Luengo et al. (systematic review, published in 2019) stated that type of performed surgical treatment and biological nature of original lesions are the most important influencing factors of local recurrence rates and furthermore metastases rates. Denosumab does not seem to affect local recurrence rates. (103) On the contrary, Chen et al. (systematic review and meta-analysis, published in 2020) declared that pre-operative use of denosumab is associated with higher recurrence risk, only post-operative denosumab therapy does not significantly increase local recurrence rates. (104) Observed higher recurrence risks in patients who underwent curettage after the use of denosumab may lead to the necessity of more aggressive curettage (e.g. in combination with cryotherapy). (105, 106)

Schedules determining loading dose and duration of neoadjuvant and adjuvant treatment of GCT with denosumab are still not well established. (67) For all patients not benefitting from primary surgical treatment, 120 mg of denosumab, given via subcutaneous injections once a week for 3 weeks, then again after two weeks, followed by continuous injections every 4 weeks, are recommended. (32, 67) Vitamin D and Calcium supplementation can complement therapy regimes. (103) In unresectable GCT, chronical use of denosumab is still not sufficiently evaluated in order to prevent progression of tumor growth while at the same time minimizing side effects. (67, 97)

Regarding recurrence of surgically unsalvageable GCT, intervals between discontinuation of denosumab and new tumor growth vary. However, there are cases in which new expansion of tumor is reported after only 7-8 months, highlighting the importance of further investigation of optimal dosis and duration regarding long-time denosumab therapy. A problem that should not be overlooked regarding chronical use of denosumab is the fact that there are diverse challenging side effects gaining importance in long-time use, for example atypical femoral fractures as well as hypophosphataemia, skin rash and mild peripheral neuropathy. (97)

The most common complications consist of nausea, bone pain, headache and fatigue. These side effects are reported in 18-25% of patients under denosumab therapy. (99, 100, 107) Beside muscular, extremity and back pain as well as arthralgia, which are commonly reported side effects, more severe complications of treatment with denosumab exist. (103) Incidences of osteonecrosis of the jaw (ONJ) are reported to be up to 6%, this severe complication seems to be dependent on the status of teeth before treatment as well as on the applicated dosis of denosumab injections. (97) Malignant transformation to glioblastoma, osteosarcoma, malignant GCT or undifferentiated pleomorphic sarcoma is described in rare cases. (105, 108-110)

Different hypotheses regarding the influence of denosumab on sarcomatous transformation exist. Inhibition of RANKL may lead to immunosuppression and raise susceptibility of nuclear oncogenes, facilitating carcinogenesis of osteosarcoma. Furthermore, it is hypothesized that through deletion of Sema3A, a gene upregulated by RANKL, denosumab may induce aberrant differentiation of osteoblasts. (105)

Hypocalcaemia can also occur after halt of denosumab injections and seems to be associated with osteopetrotic bone as well as rebound activity of osteoclasts, enforcing recommendations of electrolyte controls. (111)

1.9.5 Future possible therapeutic options

By further understanding pathological processes leading to GCT, new treatment options can be developed. One example is the investigation of diverse microRNAs (miRNAs), small RNA fragments acting within a cell without being transcribed into proteins. Some specific miRNAs have been associated with direct inhibition of specific molecular pathways: miR-127-3p inhibits COA1 gene and affects the assembly of COX 1 (cytochrome-c-oxigenase subunit). MiR-376a-3p targets PDIA6 (member 6 of protein disulfide isomerase family A) gene, which alters posttranslational processes in the endoplasmic reticulum and affects the Wnt/β-catenin pathway. MiR-126-5p downregulates MMP-13 expression and therefore inhibits bone resorption and differentiation of osteoclasts. MiR-106b is designed to target RANKL directly, suppressing osteolysis and miR-30a affects RUNX2. Safety and efficacy of these drug candidates as well as possible further indications like pancreatic, breast or bladder cancer, where some of these pathways also play a role in tumorigenesis, need to be further researched. (17, 112)

Another feature that could probably be targeted by new treatment approaches is CD33 positivity of osteoclast-like multinucleated giant cells, considering that an anti-CD33+ antibody already exists, namely gemtuzumab, which is used in treatment regimens of acute myeloid leukaemia. (67, 113)

1.10 Denosumab mediated changes regarding radiology, histology and immunohistochemistry

Denosumab therapy leads to diverse changes of radiological, histological and immunohistochemical features.

First, denosumab-related changes in radiological appearance are calcification of lesions, more defined delineation as well as a halt in progression respectively a shrinkage in size of lesion. (109) Response to treatment with denosumab can therefore also be evaluated on conventional X-ray. (25) Using a dynamic contrast-enhanced MRI (DCE-MRI) with intravenous application of gadolinium, alterations in signal-intensity curves can be seen. Before treatment, GCT lesions typically show fast and early enhancement as well as rapid washout. After therapy with denosumab, curves gradually change, eventually resembling signal-intensity curves of normal bones. (114) Original high metabolic activity of osteoclast-like giant cells can be seen on fluorodeoxyglucose-positron emission tomography (FDG PET) before treatment, high uptake of fluorodeoxyglucose should also diminish after application of denosumab. (115, 116)

Second, treatment with denosumab can alter histological findings drastically, meaning that treated lesions might not even resemble original GCT and therefore can be mistaken for various malign and benign tumors, including malign GCT. (109) Where large multinucleated osteoclast-like giant cells and mononuclear cells made up typical histologically sightings of GCT before treatment, these cell types cannot be found anymore in lesions treated with denosumab. Along with distinctive decrease of giant cells, denosumab initiates a change in appearance of neoplastic stromal cells harboring the driving mutation of GCT, H3F3A. However, these truly neoplastic cells do not disappear under treatment of denosumab, but rather present in strikingly altered appearance. (32) These distinct denosumab-induced histological changes are shown in ***Figure 6***.

Histological findings under or after treatment with denosumab can vary, ranging from cell rich areas containing oval to round neoplastic cells, or spindle cells distributed in a storiform way, containing no or only little extracellular matrix. Areas with fibrillary extracellular matrix, arranged in trabeculae or structures resembling honeycombs, constitute another pattern being described in GCT lesions after

therapy with denosumab. Presence of the different patterns seems to depend on location within the tumor, considering that more cellular areas are found in the center of lesions, whereas the periphery contains more matrix as well as merging with bone of the host. Further, areas of necrosis can be found in some samples. (117) However, distribution of each pattern varies from one patient to another. (32)

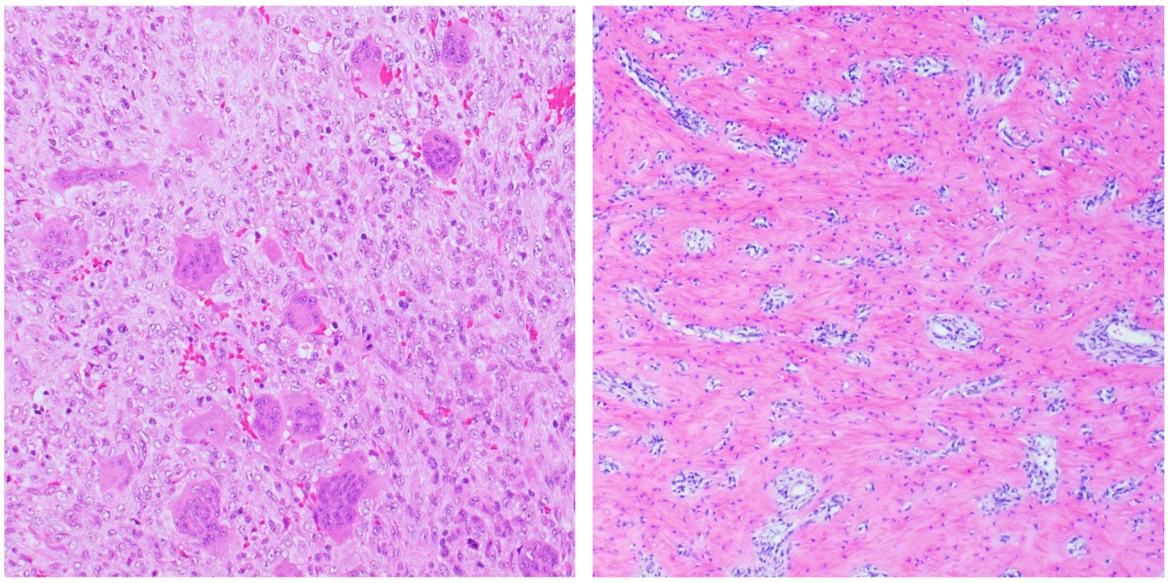

Figure 6

HE stains showing GCT before and after denosumab therapy.
Left side: GCT with multiple multinucleated giant cells. (10x magnification)
Right side: Denosumab therapy induces depletion of giant cells. New formation of reticular woven bone becomes evident. (4x magnification)
(Specimens from one of our GCT patients.)

Third, denosumab induced changes regarding immunohistochemical features highlight evidence gained through mutational analyses, leading to the conclusion that denosumab does not directly act against neoplastic stromal cells which in turn leaves recurrence of GCT after discontinuation of denosumab a problem yet to be fixed. (117, 118) Analysis of immunohistochemical staining showed that G34W and RUNX2 can diffusely be found in mononuclear cells of GCT lesions before treatment. On the contrast, multinucleated osteoclast-like giant cells are not positive for these markers. Denosumab therapy does not lead to suppression of G34W or RUNX2 considering positivity of most spindle shaped stromal cells in all cases, conforming evidence gained through mutational analyses stating that H3F3A mutations persist through therapy with denosumab. Immunohistochemical

proof highlighting the disappearance of multinucleated giant cells is a decrease in positivity for NFATc1. Before treatment, all giant cells were positive for this osteoclast marker, whereas after treatment, according to abundance of giant cells, NFATc1 decreased significantly, leaving only a minor subset of mononuclear cells positive for NFATc1. (32) Beside RUNX2, SATB2 (Special AT-rich sequence-binding protein 2) is another osteoblast marker of interest in order to study denosumab-mediated effects on neoplastic stromal cells. Comparing staining for both markers before and after treatment, consistent staining for RUNX2 but only diffuse SATB2 positivity regarding patterns with mature bone formation, becomes visible. (117) While RUNX2 marks early stages of osteoblastic differentiation, SATB2 is associated with maturation of osteoblasts, mineralization of bone and production of bone matrix. (119, 120) Less and more diffuse appearance of SATB2 may underline the hypothesis that neoplastic stromal cells constitute a defective osteoblastic phenotype only poorly associated with production of mature bone, which is seen after therapy with denosumab. (120-122) However, shortage of therapy duration might also just not provide enough time for tumor cells to develop a fully mature osteoblastic phenotype. (25)

Clinical benefits of denosumab therapy seem to be partly related to a denosumab mediated decline of angiogenesis and proliferation of GCT stromal tumor cells, considering reduced microvessel density in lesions as well as a noticeable decrease in Ki67 positivity. Reasons for these two findings are yet not fully understood. (117) Regarding reduced angiogenesis, VEGF (vascular endothelial growth factor)-mediated effects on endothelial cells play a role in regulation of microvessel density. On the one hand, VEGF enhances RANK expression of endothelial cells and therefore also increases denosumab mediated effects. (123) On the other hand, RANKL does not only induce angiogenesis by RANK, but also through endothelial nitiric oxide synthase, further leading to increased vascular permeability. (124) Concerning the decline in Ki67 labelling index, changes altering the microenvironment of neoplastic stromal tumor cells are thought to be the driving force behind reduced proliferative activity since neither inhibition of proliferation nor phenotype alteration of tumor cells through denosumab can be seen. (85, 125)

1.11 Aim of the study

The systemic use of denosumab in GCT is known to induce variable histological and clinical response along with diverse side effects. Little is yet known about long-term toxicity. Considering reports indicating short intervals between stop of denosumab therapy and tumor progression, especially in cases of unresectable GCT, further evaluation of adverse effects of long-term therapy with denosumab is needed. (97) This retrospective analysis of 54 patients with GCT including in-depth evaluation of 9 patients treated with denosumab was set out to investigate the differences in oncological outcomes as well as side effects of therapy with denosumab. One aim of this study is the evaluation of tumor database of the *Department of Orthopedics and Trauma*, *Medical University of Graz, National Center of Expertise for Bone and Soft Tissue Tumors*, including all patients treated for GCT since 1998. Furthermore, analysis of clinical, histological and radiographical response to denosumab as well as improvement of surgical therapy after neoadjuvant use of denosumab will take place. Appearance and severity of possible adverse events will be ascertained in order to generate new findings about short- and in particular long-term therapy schemata with denosumab.

2. Methods

2.1 Histology and immunohistochemistry

Histological and immunohistochemical evaluation of denosumab-mediated effects on tumor samples were investigated using several distinct methods. Samples used for this project have been provided by *Biobank Graz*, Austria. Institutional ethical approval was obtained from the Institution Review Board.
Tumoral tissues underwent fixation with 10% formalin, decalcification using EDTA till reaching a practicable hardiness, and were embedded in paraffin. For histologically evaluation, staining with haematoxylin and eosin (HE) was used. For immunohistochemistry (IHC), three- to four-micrometer thick sections underwent a procedure specific for each desired antibody. Being the driving mutation in GCT, an antibody directed against H3.3 G34W (Clone RM263, a rabbit monoclonal antibody, RevMab Dianova) was used to verify the diagnosis of GCT. As declared by Datashield/manufacturer information, tissues were automatically processed by VENTANA® BenchMark ULTRA platform. First, heating for about 1 h at 70°C was performed, followed by prepping using „CC1 mild“ for 36 min, manually titration of 100 µl „titration antibody 995“ (1:500 dilution), 32 min of incubation as well as a program named „ultra wash“ using ULTRA KIT as detection medium. Second, counter staining with haematoxylin for 8 min in order to visualize cells not positive for this antibody, and bluing with a so called „Bluing Reagent“, were performed. To visualize antibodies bound to their target, DAB (Diaminobenzidin-Tetrahydrochlorid) is frequently used in IHC procedures. In this case, the iVIEW DAB Detection Kit from Ventana was used to detect the rabbit IgG antibodies (like clone RM263 bound to the antigen Histone H3.3 G34W). Location of the specific antibody was detected by a secondary, biotin-conjugated antibody, followed by conjugation of streptavidin-HRP (a streptavidin enzyme) with the secondary antibody, whereas final visualization was accomplished by application of hydrogen peroxide substrate and DAB, leading to the characteristic brown color. Nuclear staining was considered positive when the tumor cells showed moderate to strong positivity.

2.2 Molecular analysis

Mutational analysis (MA) was used to verify diagnoses in challenging cases. DNA was extracted from formalin-fixed, paraffin-embedded (FFPE) material using 5-8 unstained, 10 µm thick sections from a representative block. Macro dissections were performed with a scalpel to enrich for tumor content. According to manufacturer's instructions, DNA was isolated using the Maxwell RSC DNA FFPE kit, quantified by picogreen fluorescence and 20 ng of DNA were used to perform next-generation sequencing (NGS)-based anchored multiplex PCR technique (Ion Torrent, MUG Bone Panel - searching for mutations in the *IDH1*, *IDH2*, *H3F3A, H3F3B*, *EXT1*, *EXT2*, *p53* (Exon 4-10) genes). The analysis was performed in the *Laboratory for Diagnostic Genome Analysis, Diagnostic and Research Institute of Pathology, Medical University of Graz*. Mutations were annotated following the recommendations of the Human Genome Variation Society (HGVS). (126)

2.3 Statistical analysis

Fifty-four patients with giant cell tumors of bone treated at the *Department of Orthopaedics and Trauma, Medical University of Graz (Austria)* between 1998 and 2020 were included into the retrospective analysis. Institutional ethical approval was obtained from the Institutional Review Board. Epidemiological evaluation was based on gender, date of birth and age at diagnosis of all selected patients. Reason for admission as well as character and duration of symptoms prior to first medical contact were documented, although these informations were not reasonably ascertainable in all cases. Side of the lesion and location within bone or joint, size, metastases (when present), histology, IHC and MA were documented as tumor specific characteristics. Of note, used IHC analysis varied due to year of diagnosis, considering that the mutation specific antibody was available after 2017. To assess therapy schedules, date and type of surgery, margins of tumor resections and character of neoadjuvant as well as adjuvant therapy schemata were collected. With respect to surgical margins, samples were grouped into three categories: 1) R0 - wide resection, depictured by tumor-free margins of at least 2 mm; 2) R1 - marginal resections (0.1 – 2 mm distance) and 3) R2 - macroscopically tumor on the margin (intralesional resections). Further documented data included patient-ID, date of diagnosis, local recurrence, and date of last orthopaedic follow-up. In cases where local recurrence occurred until the last follow-up, date and treatment of recurrence were ascertained. Therefore, three groups were defined: Group 0 did not show local recurrence at any time, Group 1 developed local recurrence and remission due to received therapy and Group 2 was characterized by existing recurrence.

2.3.1 Inclusion criteria

In order to verify the diagnosis, HE-stained sections of all available cases were reviewed by PD Dr. Iva Brcic, a specialist for bone and soft tissue pathologies, and Lisa Jernej. Previously performed IHC stainings were reviewed as well and most commonly included SATB2, p63, and S100. Furthermore, an additional staining with H3.3 G34W was performed in every case diagnosed before 2018 were material available for analysis was present.

From 2018, all tumor samples were routinely stained using an antibody against H3.3 G34W. Out of 70 patients potentially available, 54 were finally included in this retrospective analysis. Staining with H3.3 G34W and mutational analysis were performed in 30 and 11 cases, respectively.

2.3.2 Statistical program

Data collection and statistical analysis were performed by using Microsoft Excel for Microsoft 365, Version 2012 and IBM SPSS Statistics, Version 26. Descriptive analysis was used to ascertain frequencies of categorial or binary variables (e.g. administration of neoadjuvant therapy: yes / no). Detailed analysis of continuous variables (e.g. size of the tumor) took place via explorative analysis and consisted of determination of the median, mean, 95% confidence interval, minimum, maximum, variance and standard deviation. The relationship between two categorial variables was evaluated with Pearson's Chi Square Test (X^2-Test). One-way ANOVA Test was used to determine if there is a relationship between the frequency of local recurrence and size of the lesion (grouped in 3 categories).

2.4 In-depth analysis of patients treated with denosumab

Ten patients between 2009 and 2020 underwent systemic therapy with the human monoclonal antibody denosumab. One patient was excluded from the analysis because diagnosis of GCT could not be verified retrospectively.
Each patient`s history was analyzed by in-depth evaluation of doctor`s letters, radiological findings, surgical reports as well as pathological results. Of note, the amount of available information varied significantly. Missing information was mostly caused by fluctuation of patients. Due to the rareness of GCT, patients were often treated at different centers and even in different countries, or in the beginning only obtained a second opinion and then decided to continue therapy at the *Department of Orthopaedics and Trauma* in Graz.

3. Results

3.1 Work flow of enrolment and exclusion of patients with histological, immunohistochemical and mutational findings

Analysis of tumor databank revealed 70 patients with diagnosis or differential diagnosis of GCT. Patients with initial diagnosis or local recurrence (LR) after 2018 were routinely assessed using IHC and MA (n=11). Patients with untypical clinical or radiological features and unavailable material for IHC were excluded (n=7). In 23 cases, specimens were available. IHC with H3.3 G34W was performed in 19 cases: in 14 cases moderate to strong nuclear positivity was observed, in 5 cases reaction was negative. One patient was excluded due to untypical clinical features. Regarding the remaining 4 patients with GCT-like histological features and negative staining for H3.3 G34W, MA was performed. In all 4 cases, no mutations in H3F3A gene specific for GCT were found. Therefore, differential diagnosis of brown tumor due to hyperparathyreoidism was suggested to be the most likely diagnosis. Of all available specimens, untypical clinical features, IHC and MA lead to exclusion of 9 patients. Finally, 54 patients with verified diagnosis of GCT were enrolled in the statistical analysis of clinicopathological data, as can be seen in ***Figure 7***.

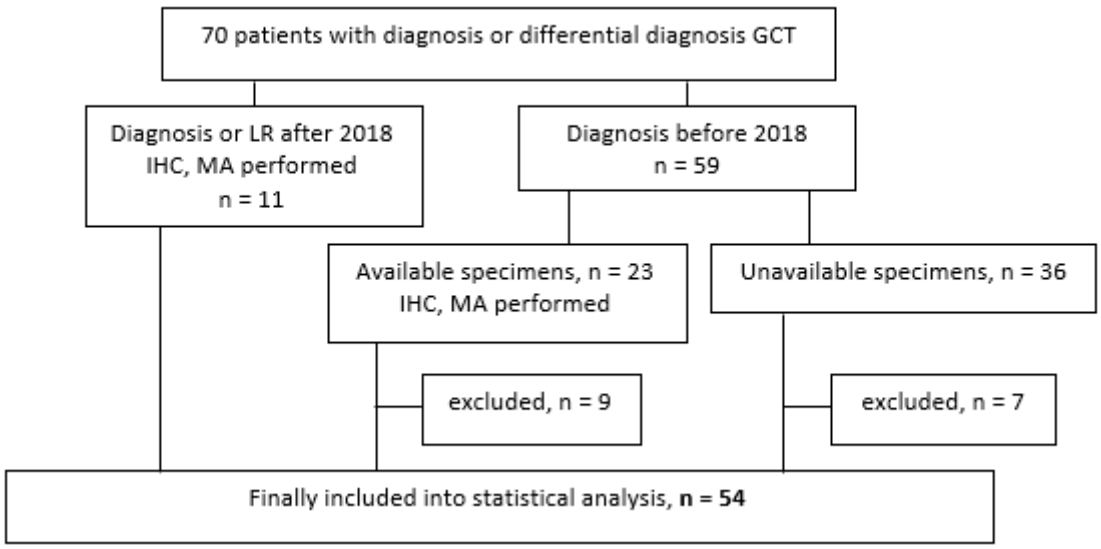

Figure 7 *Flow chart depicting inclusion criteria and performed immunohistochemical staining for H3.3 G34W (IHC) and mutational analysis (MA).*

Macroscopically, most of GCTs presented as well demarcated lesions. Histological reevaluation took place via conventional HE staining. Typical histological features included neoplastic mononuclear stromal cells admixed with non-neoplastic multinucleated osteoclast-like giant cells. The number of nuclei in one giant cell varied from only a few up to almost 50. IHC with SATB2 showed positive nuclear staining in neoplastic mononuclear cells. On the contrary, multinucleated osteoclast-like giant cells were negative (***Figure 8***).

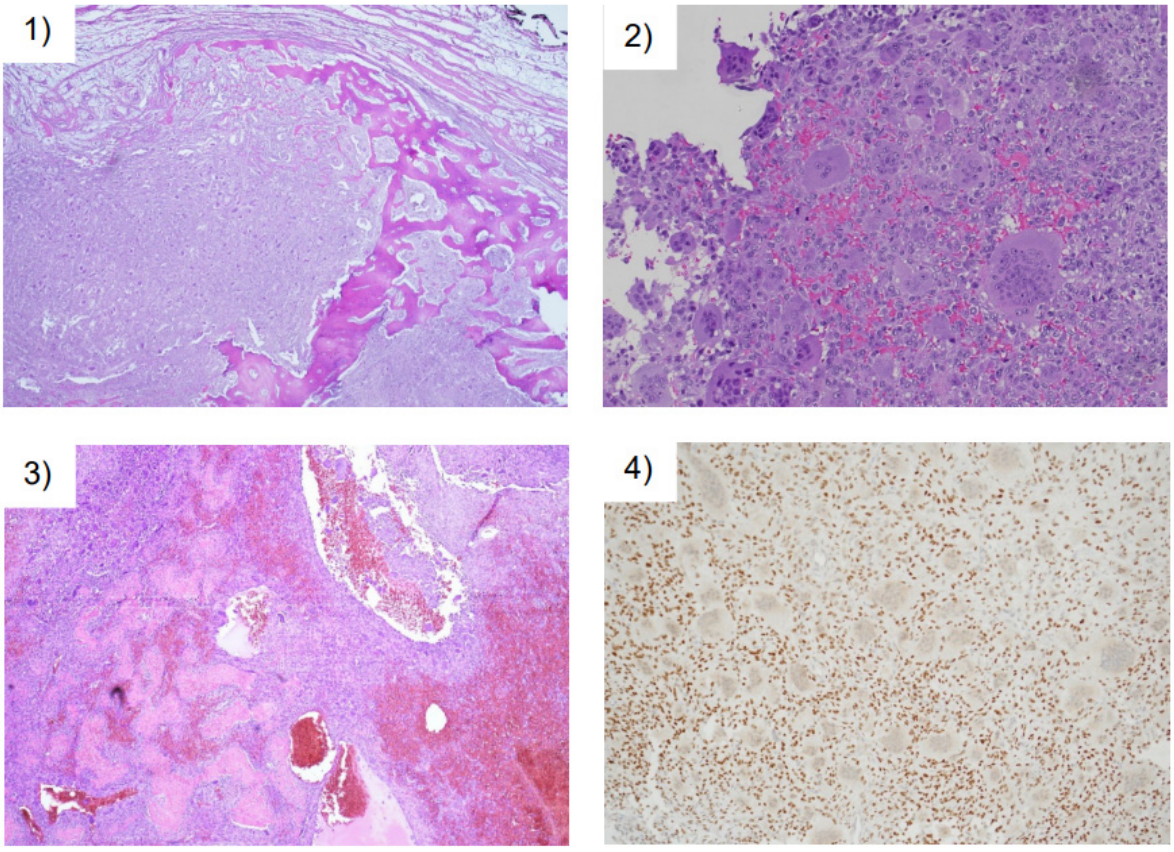

Figure 8 *Conventional GCT lesions*

1) Overview image of GCT, showing a relatively well circumscribed lesion. (2x magnification)

2) Tumor is composed of neoplastic mononuclear cells and multinucleated osteoclast-like giant cells. One giant cell contained at least 45 nuclei. (10x magnification)

3) Extensive haemorrhage within the tumor. (4x magnification)

4) IHC with SATB2. The neoplastic mononuclear cells showed positive reaction. On the contrary, multinucleated osteoclast-like giant cells were negative. (10x magnification)

Overall, 30 IHC using a specific antibody against H3.3 G34W, the most common mutation in GCT, were performed. IHC and histological evaluation of therapy response to denosumab can be seen in ***Figure 9***. Pictures 1) – 4) show specimens originating from *Patient 1*, a 52-year-old woman with a GCT lesion in the left elbow, whose medical history is described in the chapter of case reports in this diploma thesis.

Picture 1) highlights that only neoplastic mononuclear stromal cells express the mutation H3.3 G34W. Neoplastic cells showed positivity as opposed to reactive osteoclast-like multinucleated giant cells. By comparing picture 1) and 2), survival of neoplastic stromal cells through therapy with denosumab becomes evident. Positive reaction is shown on both pictures, demonstrating the presence of neoplastic cells harboring the mutation H3.3 G34W before as well as after 6 months of therapy with denosumab. Specimen 3) shows a well restricted lesion with typical histological therapy-associated alterations: depletion of giant cells and formation of new reticular woven bone. Denosumab treated lesions showed areas containing more osteoid and bone formation and more cellular areas, as specimen 4) shows. Of note, neoplastic cells found after therapy with denosumab often exhibited a bland nature without nuclear atypia.

Picture 5) and 6) originate from *Patient 3*, a 21-year-old man with GCT at the epicondylus radialis of the distal right humerus. Specimen after 3 months of therapy with denosumab can be seen in image 5). Cellular areas were surrounded by new bone formation, resembling a mixture of patterns seen in specimen 4). IHC with an antibody directed against H3.3 G34W of this lesion is shown in picture 6). Again, neoplastic cells showed positive nuclear staining after therapy with denosumab in contrast to negative multinucleated osteoclast-like giant cells.

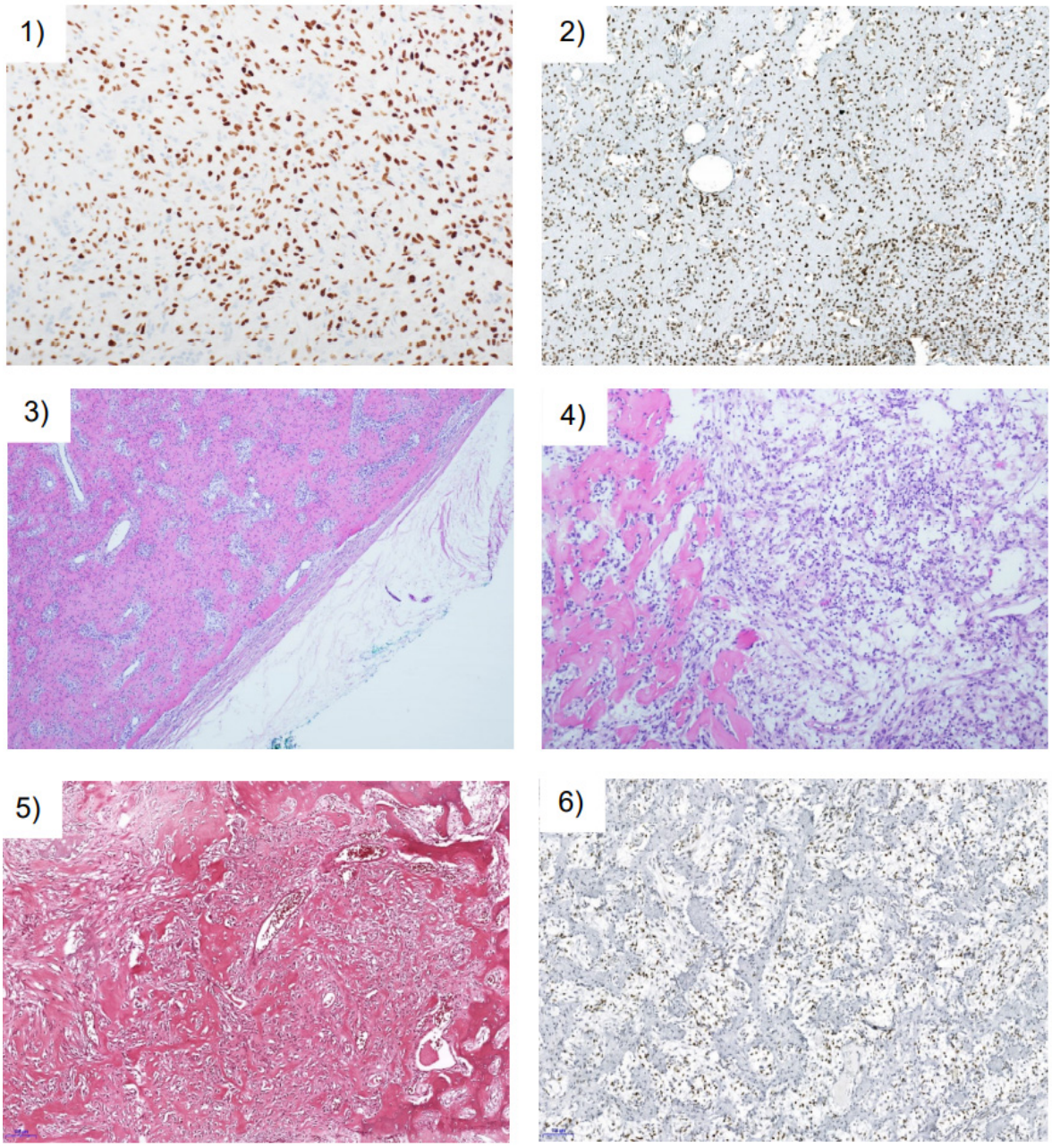

Figure 9 Staining using an antibody against H3.3 G34W and therapy-associated changes of GCT

1) IHC before therapy with denosumab. (20x magnification)

2) IHC after therapy with denosumab. (10x magnification)

3) HE stain after therapy with denosumab for 6 months. (4x magnification)

4) More cellular regions containing bland neoplastic cells. (10x magnification)

5) HE stain after therapy with denosumab for 3 months. (10x magnification)

6) IHC after therapy with denosumab. (10x magnification)

3.2 Results of statistical analysis

3.2.1 Patient characteristics

Among the 54 analyzed patients with GCT, 28 (51.9%) were female and 26 (48.1%) were male. Mean age at diagnosis was 37.9 years (ranging from 16 - 80 years, 95% CI: 33.6 – 42.2 years). Duration of symptoms prior to admission was ascertainable in 28 cases and ranged from 0 months up to 54 months. The mean time of symptoms was 5.8 months, 17.9% of the patients described symptoms for less than 1 month, and 78.6% described symptoms for 6 months or less. One single patient suffered 54 months from long-time unidentifiable back pain due to GCT located at L2. Duration of symptoms did not significantly differ neither regarding gender (p=0.431; X^2-Test) nor regarding age at diagnosis (p=0.590, X^2-Test).

Most patients (86.5%) declared to have experienced pain prior to admission, whilst 8.1% had no symptoms. Increase in size or pain as well as increase were described by a minority of the patients (***Figure 10***).

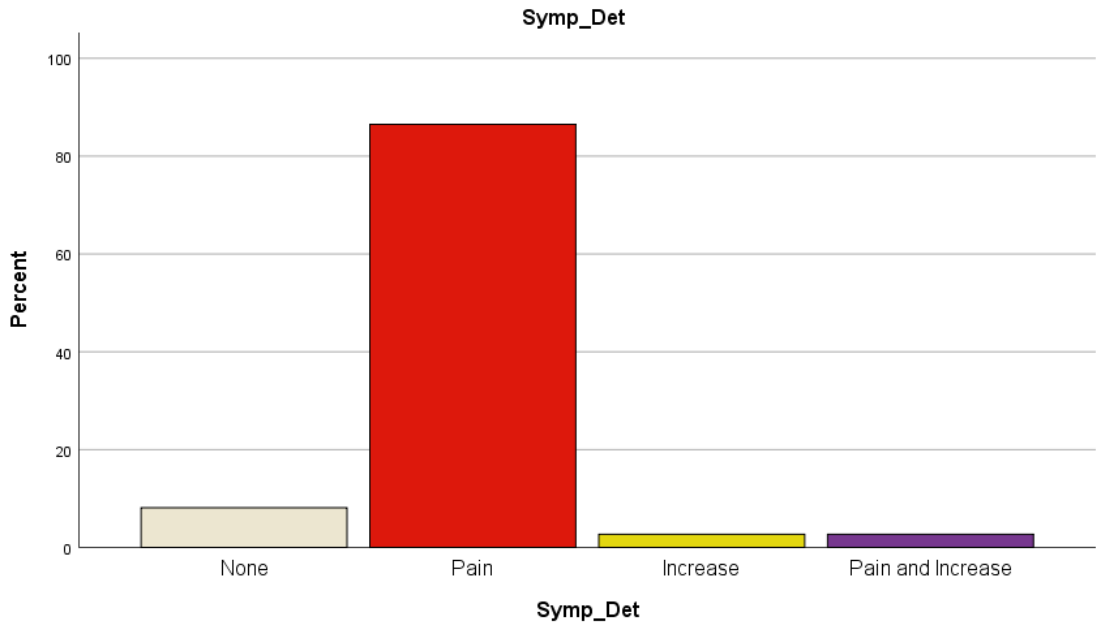

Figure 10 *Details regarding declared symptoms prior to admission.*

The three major reasons for admission were pain (73.2%), pathologic fractures (14.6%) and incidental finding (4.9%, meaning that a conspicuous lesion became apparent in a radiology performed out of other reasons). Two patients had already been diagnosed with GCT and obtained a second opinion from the *Department of Orthopaedics and Trauma* in Graz. One single case presented with swelling of the affected area (***Figure 11***).

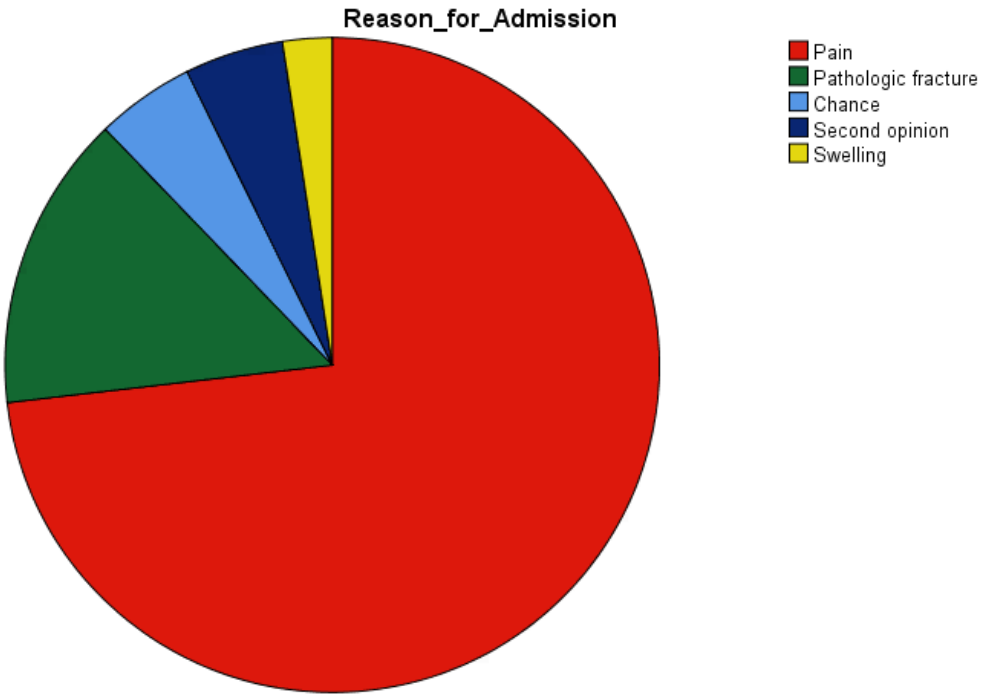

Figure 11 *Reasons forcing patients to consult orthopaedic ambulances.*

3.2.2 Tumor specifications

Interestingly, 59.3% of GCTs were located at the left body side, whereas only 38.9% were located on the right side. One tumor was not assignable to one side (L2). Altogether, 98.1% of GCTs were singular lesions, one patient showed multiple lesions at the wrist. Two patients (3.7%) had lung metastases confirmed by biopsy. Size of the tumors ranged from 1 cm up to 17 cm, mean size was 5.1 cm. More than half of the tumors measured less than 5 cm (63%). Split by anatomical location, GCTs located at the knee were larger (mean size 6.2 cm) than those at the elbow (3.4 cm). Notably, any tumor larger than 10 cm in size had been located in the knee region.

As ***Figure 12*** shows, the majority of GCTs (55.6%, n=30) were located at the knee joint (distal femur: medial condyle, lateral condyle or intercondylar; proximal tibia and head of fibula), followed by 13% (n=7) located at the distal radius or wrist. Further 7.4% (n=4) were located at the elbow (distal humerus: medial or lateral epicondyle; proximal radius) as well as 7.4% (n=4) at the distal tibia and talus. Only 5.6% (n=3) occurred at the hip (os sacrum, os pubis, os ischium, os ilium) and at the proximal humerus (n=3). Rare locations were the proximal femur (n=2) and the lumbar spine (n=1).

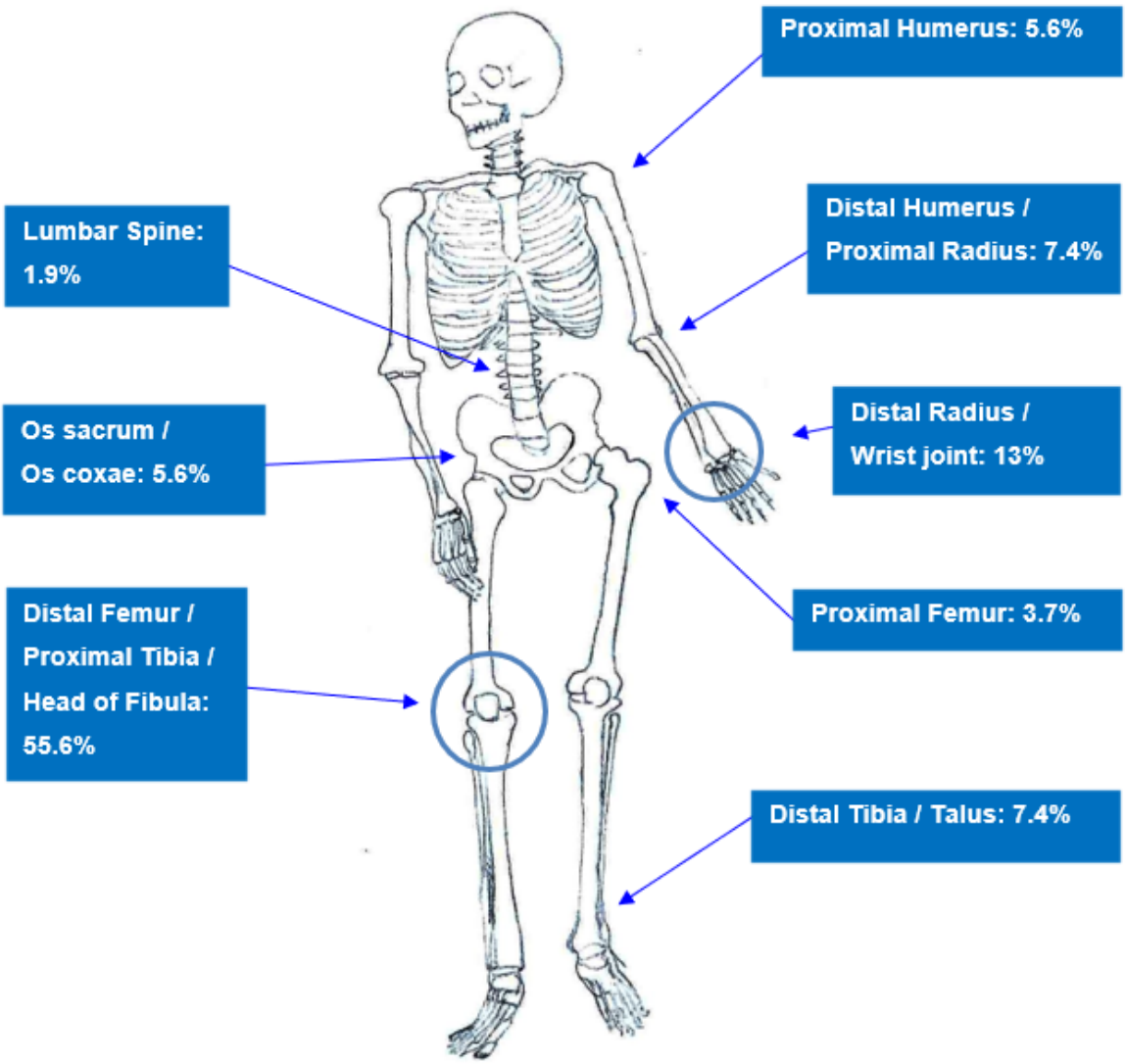

Figure 12

Locations of GCTs. Side of the body was not considered in this figure.

3.2.3 Therapy schemata

Neoadjuvant treatment

Neoadjuvant therapy was applied to 2 patients (resembling 3.7% of all patients). Denosumab was used in one case prior to first operation due to difficult anatomical location (L2). Zoledronic acid was applied once every 3 months to another patient.

Surgical therapy

All patients underwent surgery with initial curative intent. The number of operations performed in each patient was dependent on outcome after operation (re-operations due to pain, movement restriction, loosening of screws or implants) and appearance of local recurrence. Most patients (59.3%; n=32) underwent 1 operation, 25.9% needed 2 operations (n=14). Three or more operations were necessary in 14.8% of cases (n=8) (***Figure 13***). Margins of tumor resections (R0, R1 or R2) were ascertainable in a minority of patients (14.8%, n=8) because curettage combined with local adjuvants was the most often used surgical therapy.

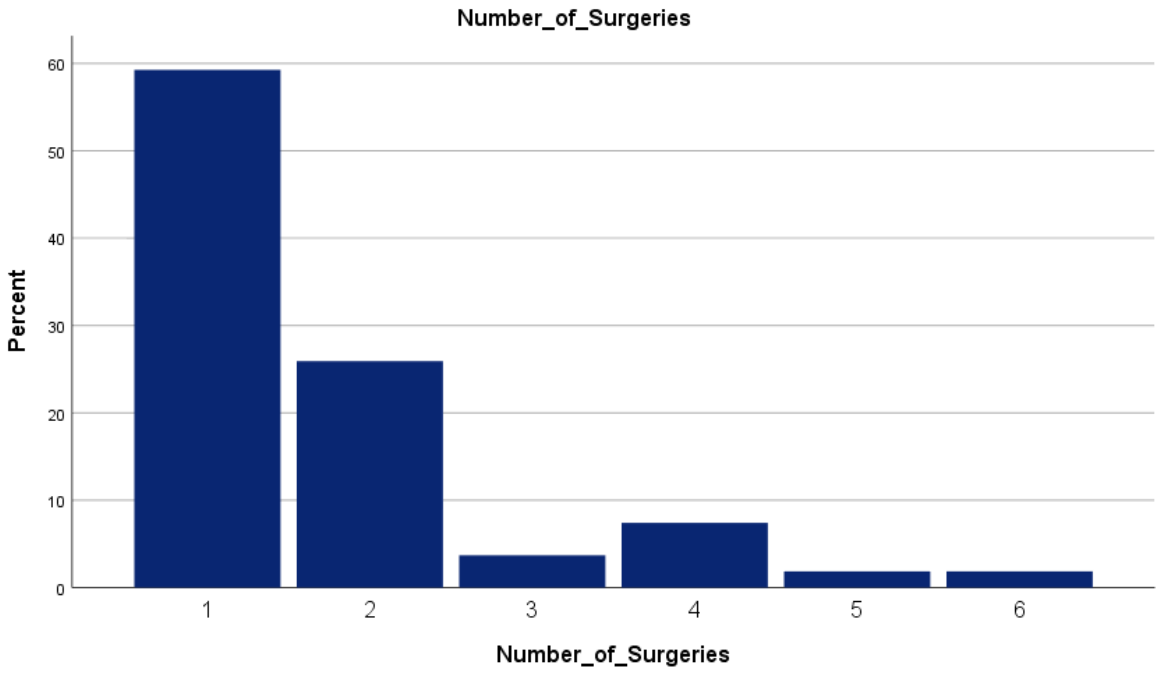

Figure 13 *Total number of surgeries of each patient*

Adjuvant treatment

Adjuvant treatment was administered in 18.5% of the patients. Overall, 70% of adjuvant therapies consisted of denosumab alone.

Further, radiotherapy in combination with denosumab, radiotherapy alone and zoledronic acid was used as adjuvant therapy, as ***Figure 14*** shows.

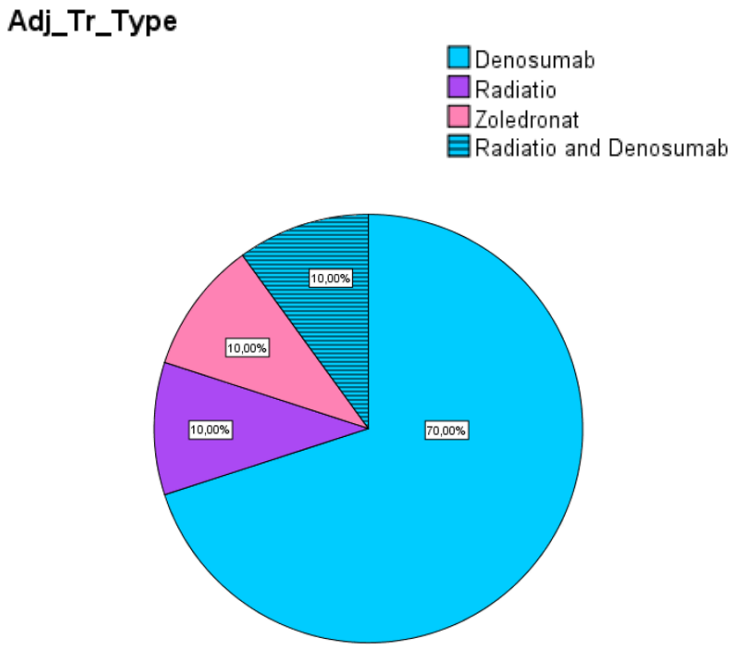

Figure 14 *Different types of adjuvant treatment*

Local recurrence

Three quarters of the patients (74.1%) did not show any signs of local recurrence until the last follow-up, whereas 25.9% (n=14) developed local recurrence. Of all patients, 13% (n=7) had one local recurrence, 5.6% (n=3) had two and in 7.4% (n=4) tumor recurred for 3 times. There was no significant correlation between the development of local recurrence and size of primary lesion (size grouped in 3 categories: < 3.1 cm, 3.1 – 4.5 cm and > 4.5 cm, p=0.904, one-way ANOVA Test). Signs of local recurrence were diverse. Some patients complained about swelling, pain or sensomotoric disorders. In other cases, imaging techniques (X-ray, CT and/or MRI) showed suspicious lesions. Mean time from removal of the primary lesion to the appearance of first local recurrence was 46.4 months, ranging from 1 to 312 months (0.1 - 26 years, 14 cases). In half of the patients with local recurrence, tumors recurred within 11 months. Duration from first to second local recurrence lasted on average 25.9 months (range: 3 – 63 months, 7 cases) and the mean interval between second and third local recurrence was 6.5 months (range: 4 – 8 months, 4 cases).

Therapy of recurrence consisted of re-operation and / or the use of denosumab. At the *Department of Orthopaedics and Trauma* in Graz, difficult cases were discussed at multidisciplinary tumor board sessions, where individual parameters of patients (including age, comorbidities, living conditions) and tumors (histology, size, aggressivity) were considered in order to find the presumably best therapy approach.

The decision to re-operate was made in 53.8% of all cases of recurrence. Denosumab was used in 38.5% in addition to re-operation and in 7.7% as single therapy approach. ***Figure 15*** gives an overview of all cases affected by local recurrence.

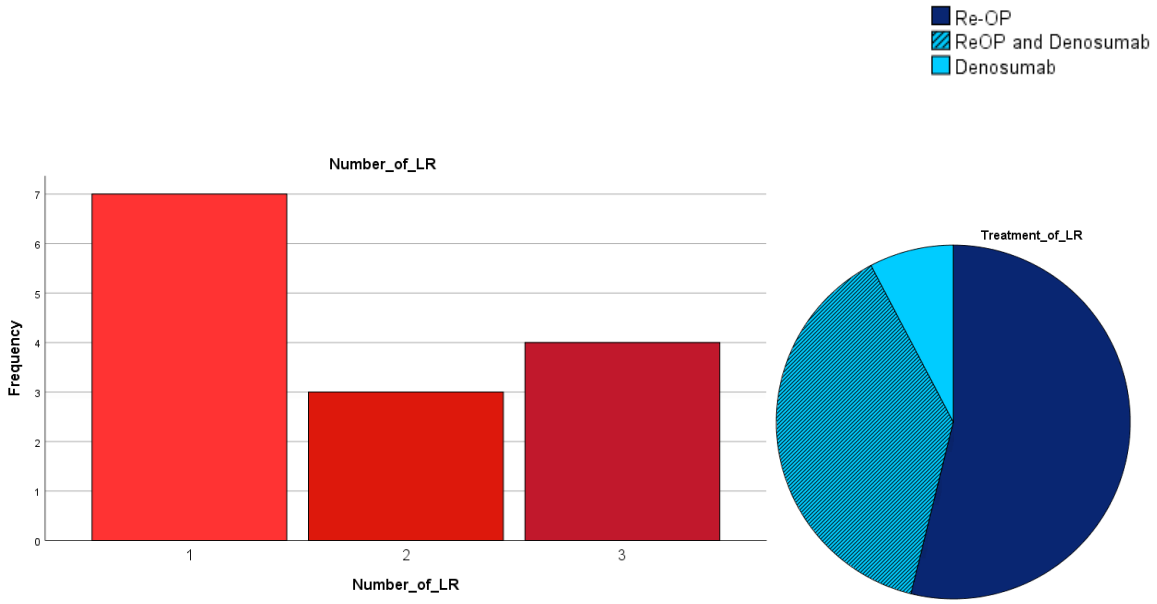

Figure 15

The number of patients affected by one, two or three local recurrences are shown on the left side of the figure. On the right side, different therapy approaches in case of local recurrence are visualized.

Follow-up

Mean follow-up was 68.9 months (range: 0 to 316 months). Each patient was allocated to one of three categories due to their outcome: 74.1% had no local recurrence at all, 20.4% developed recurrence and remission after therapy and 5.6% still showed existing local recurrence until the last follow-up.

3.3 Case reports: Patients treated with denosumab

3.3.1 Patient 1

In May 2014, a 52-year-old woman presented to the orthopaedic outpatient clinic for consultation complaining of pain in the left elbow. X-ray of the affected joint showed an osteolytic lesion in the epiphyseal region of distal humerus which also included cortical destruction. Open biopsy of the conspicuous lesion showed fragments of a giant cell rich lesion with focal production of osteoid, declared as primarily giant cell tumor of bone (differential diagnoses: reparative giant cell granuloma, brown tumor associated with hyperparathyreoidism, aneurysmatic bone cyst, fibrous defect of corticalis or chondroblastoma). Consistent with tumor board decision, the first operation consisted of curettage and compound osteosynthesis with 5-screw-LCP-plate and use of osteosynthesis material. The surgery went uneventful as well as post-operative recovery. The histopathological examination of the removed mass was consistent with GCT. Follow-up included clinical and radiological controls every 3 months and intensive physiotherapy since the patient was repeatedly complaining about movement restriction. Almost a year after the first admission (April 2015), the patient presented again, describing recent pain dorsomedial at the elbow. Radiography showed anew an osteolytic lesion highly suspicious of local recurrence.

At tumor board, decision was made to start therapy with denosumab/Xgeva® because operation was expected to be mutilating. After dental clarification because of the known side effect of osteonecrosis of the jar (ONJ), application of denosumab followed. The patient furthermore complained of pain, also at night, but no specific side effects that could be attributed to therapy with denosumab. During 6 months under denosumab therapy, radiology showed no progression of the tumor. After 6 months, break of 2 screws became evident in CT and the patient described in addition an increase in pain, especially under load and at night, and numbness. Open biopsy took place, followed by the second operation consisting of revision, extraction of metal, recurettage, refilling of the defect with Palacos and plating. The patient underwent only 2 months later the third operation (resection of the distal humerus, implantation of endoprosthesis Mutars totally cemented) due to persistent pain, movement restriction and aseptic loosening of screws.

Seventeen months after the first local recurrence, CT showed a nodule in the soft tissue medial at the left elbow region, resembling a local recurrence. Review of the case in the tumor board lead to 1) CT scan of the thorax in order to exclude lung metastases, 2) second therapy with denosumab for 6 months and 3) planned resection of the mass after neoadjuvant denosumab therapy. Again, dental consultation took place before start of therapy with denosumab, as well as prescription of Cal-D-Vita 2x1 and regularly controls of serum calcium levels. Again, no tumor progression was ascertained under denosumab therapy. Partly calcification of the soft tissue lesion was shown in radiography (***Figure 16***).

Figure 16
Images of the left elbow region.
On the left side, the primary lesion can be seen: an osteolytic lesion in the epiphysis of the distal humerus with cortical destruction.
On the right side, integrated endoprosthesis as well as second local recurrence is shown: a nodule in the soft tissue medial, close to the N. ulnaris, partly calcificated after three months of therapy with denosumab.

The fourth operation took place 6 months later. At this time, the patient showed ascending pain in the region of N. ulnaris, where the nodule (measuring 6 cm in diameter) was located. Histopathology of the removed tissue confirmed local recurrence, as ***Figure 17*** shows.

Not a year later, the patient presented again with increasing pain and swelling. MRI scan showed a 3 x 3.5 cm measuring recurrence in the soft tissue adjoining the M. pronator teres (Caput humeri). Again, third therapy with denosumab was started in consensus with tumor board decision. After 3 months of neoadjuvant therapy, fifth operation (marginal resection of local recurrence) took place. Until the last follow-up (September 2020), the patient complained about pain in the affected area, and thus is under multidisciplinary pain management. However, no signs of further local recurrence were apparent.

Summarized, over a time period of more than 6 years, this patient suffered 3 local recurrences, 3 therapies with denosumab (two times for 6 months, the third time for 3 months – in total 15 months) and 5 operations. No side effects of denosumab were reported. Radiologically, calcification of the lesions was found. However, pain did not decrease and local recurrence occurred under denosumab therapy, increasing the risk of secondary malignant transformation and metastases.

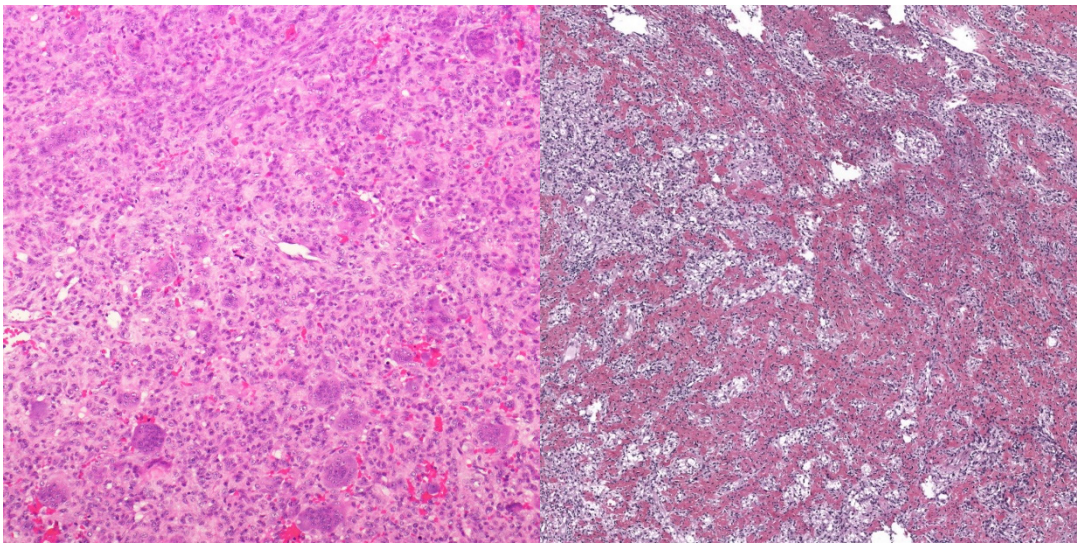

Figure 17

HE staining of primary GCT can be seen on the left side: many osteoclast-like giant cells containing a high amount of nuclei and neoplastic mononuclear cells can be found. (10x magnification)

On the right side, local recurrence after therapy with denosumab is shown. The absence of multinucleated giant cells is clearly visible. (4x magnification)

3.3.2 Patient 2

In August 2013, a 27-year-old man underwent extirpation of a tumor located at the left distal femur in Bagdad. Histology of the removed mass (measuring 8.5 x 6 cm) was described as an aneurysmatic bone cyst with few foci containing multinucleated giant cells as well as spindle-shaped cells in the stroma, leading to the differential diagnosis of GCT.

Almost one and a half years later, in 2015, the patient presented at the *Department of Orthopaedics and Trauma* in Graz complaining of swelling and pain in the same region. X-ray showed cement filling as well as a distinct darkening in the soft tissue surrounding the lateral condyle and the distal end of the left femur. MRI scans indicated a partly intraosseous, but mostly extraosseous located polycystic lesion (craniocaudal length: 9 cm, width: 2.5 cm). Skeletal scintigraphy can be seen in ***Figure 18***. Pronounced hyperperfusion at the distal femur was shown, the rest of the body was inconspicuous.

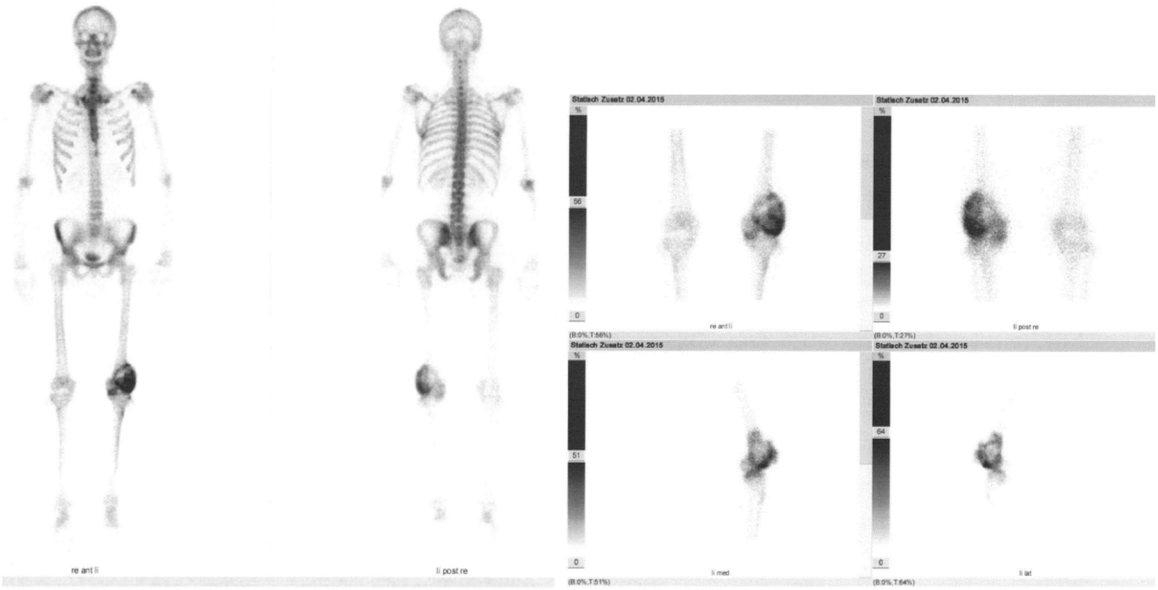

Figure 18 *Bone scan of the whole body as well as focused on the suspicious left femur.*
Significant pathological tracer uptake was most intense at the lateral and caudal proportion of the suspicious lesion, in total affecting the entire lateral condyle, the metaphysis and partly also the medial condyle. Maximal relative storage was 6.5 at the left distal femur, corresponding to an intermediate - high grade metabolically active process in the bone.

Incisional biopsy followed and histopathological analysis was consent with local recurrence of GCT. Additionally, CT of the thorax showed several subpleural located nodules in the lower lobe of the right and left lung, the biggest nodule measuring 1 cm in diameter. Differential diagnoses included post-inflammatory granuloma, carcinoma of the lung or GCT metastases. Also, 2 nodules of 1.5 cm length were described in the spleen (primarily interpreted as normal variants according to accessory spleens).

Tumor board decision fell on therapy with denosumab for one year and regular radiographical controls.

After 3 months, the lung nodules seemed to shrink in size. However, 6 months after start of the therapy, lack of response to denosumab became apparent: The lesion in the femur did not shrink in size, although radiography indicated little ossification. The lung nodules definitely showed no remarkable reduction in size. Nevertheless, therapy with denosumab was continued in order to reach further ossification and in the end lasted for 14 months. The patient underwent the second operation almost three years after the first. Wide resection and implantation of an endoprosthesis of the femur (Mutars) was performed.
After the operation, the patient complained about painful soft tissue swelling 10 cm cranial of the knee joint, but MRI scan did not show any signs of local recurrence. Dignity of the lung nodules never seemed to be fully cleared up. This can be explained by lack of increase in size as well as difficult socio-economic status of the young patient. Until the last follow-up in 2017, no further events were documented.

In conclusion, it can be said that this male patient underwent one local recurrence, one therapy with denosumab lasting for 14 months and 2 operations. Lung nodules with unclear dignity did not decrease significantly under denosumab therapy. Local recurrence remained the same size but showed ossification after prolonged therapy duration. No side effects of denosumab were reported.

3.3.3 Patient 3

In January 2013, a 21-year-old man complained about pain at the right elbow. X-ray showed an osteolytic lesion, measuring 3 cm in diameter, consuming almost the entire epicondylus radialis of the distal right humerus. MRI scan showed uptake of contrast media and break through as well as a small soft tissue component ventral of the lesion. Open biopsy was made, the extracted tissue was consistent with GCT. The first operation consisted of curettage, jet lavage, use of phenole, reconstruction with compound osteosynthesis, filling with palacos and plating with a 5-screw-LCP-plate on the lateral side of humerus.

Movement restriction caused by mechanical irritation of the surrounding tissue due to a too long screw occurred. Further, CT scans showed signs of cortical destruction. Therefore, the second operation followed 8 months after the first in order to remove the most distal screw and to histologically examine the questionable osteolysis. Pathological evaluation of the removed mass confirmed local recurrence. A year after the first operation, complete excision of recurrence took place. Start of therapy with denosumab or second-line radiotherapy were discussed at tumor board session. No action was decided due to lack of information about therapy with denosumab among patients of such young age. Four years later, the patient presented again with pain and swelling since a work accident. CT scan showed a lesion measuring 12 x 3 x 4 cm with irregular margins at the right elbow. MRI scan also indicated a soft tissue component. Neoadjuvant therapy with denosumab was started with 120mg sc. every 4 weeks with additional injections at day 8 and 15 in the first month. Aim of the therapy was to better define the boundaries of this second local recurrence. Vitamin D and calcium were also prescribed. After 3 months, the patient showed good response to denosumab and did not report any side effects. Calcification of the rim surrounding the lesion was evident. The fourth operation included the resection of the distal humerus and implantation of a tumor-endoprosthesis (Mutars) at the right elbow. Histological evaluation of the resected bone and soft tissue mass was consent with local recurrence and therapy-associated changes. Margins were described as tumor-free.

Until the last follow-up (almost 2 years after the fourth operation), the patient complained about symptoms during supination and pronation of the elbow and arthrosis of the distal radio-ulnar joint. However, flexion and extension were described as completely pain-free. No other complaints were documented.

To sum it all up, this male patient underwent 2 local recurrences and 1 neoadjuvant therapy with denosumab (lasting 3 months) as well as 4 operations. Response to therapy with denosumab was satisfactory and no side effects were reported.

3.3.4 Patient 4

In 2015, a 32-year-old woman underwent intralesional resection of GCT located in the distal radius of the right wrist joint in Tuzla, Bosnia-Herzegovina. Reconstruction with autologous fibula took place. Multifocal local recurrence occurred only 3 months later, involving the os lunatum, os scaphoideum, os capitatum as well as the neoradius. The patient obtained a second opinion from the *Department of Orthopaedics and Trauma* in Graz. Recurrence measured 5 x 3 cm, implantation of the fibula lead to a protuberance of 1.5 cm according to the carpus.

Tumor board decision fell on neoadjuvant therapy with denosumab for 3 months followed by reevaluation of surgical therapy options. Therapy schemata consisted of 120mg denosumab each on day 0, 8, 15, 30, MRI scan on day 45 and again 120mg denosumab on day 60 and 90. Unfortunately, the patient misunderstood the schemata and injected 120 mg denosumab additionally on day 45. Radiography showed shrinkage in size of the multifocal recurrences. Therefore, prolonged therapy duration was decided. In the end, therapy lasted for 7 months.

The second operation included resection of the recurrence, arthrodesis of the wrist and reconstruction with allograft. Post-operative recovery was uneventful; histology was consent with local recurrence of GCT with changes due to denosumab.

Six months later, the patient presented again with local recurrence in the soft tissue. MRI scans showed nodules palmar at the wrist (superficially located near the tendons of the flexors). Again, decision fell on neoadjuvant use of denosumab for 3 months, leading to a decrease in size of the soft tissue recurrences. The third operation consisted of marginal resection. Accompanying synovitis caused little pain.

More than one and a half years later, third local recurrence occurred according to a painless swelling of the wrist, which increased over only two weeks and measured 2 cm. Incisional biopsy of the lesion confirmed soft tissue recurrence of GCT. Forth operation (marginal resection) followed.

On the last follow-up (3 months after the fourth operation), postoperative recovery was uneventful.

It remains to be said that this patient developed 3 recurrences and underwent 2 therapy schedules with denosumab, the first lasting for 7 months and the second for 3 months (10 months in total). No side effects were reported during denosumab therapy and lesions showed reduction in size. Preserved movement in the elbow but arthrodesis of the wrist were the results of 4 operations. However, no significant pain problem was documented.

3.3.5 Patient 5

This 55-year-old man presented in July 2012 with pain at the lower leg to the orthopaedic outpatient clinic in Salzburg. Performed biopsy was consent with GCT located at the distal tibia. The first operation consisted of curettage, use of phenol and filling with CTBA granula. Local recurrence became evident only 5 months later, radiography showed visible dissolution of the implanted artificial material. Therefore, second operation took place (curettage, use of phenol, filling with cement). Again, remission lasted only for a few months until second local recurrence cranial and medial of the first became apparent. Additionally, X-ray of the thorax showed distinct lung metastases, confirmed by CT-guided biopsy.

Nine months after first medical contact, specimens were sent to the *Department of Orthopaedics and Trauma* in Graz in order to obtain a second opinion. This case is exceptional due to focal significant high proliferative activity, ascertained by immunohistochemical staining for Ki-67. Up to 7 mitoses per 10 HPF (high power field) were described. Samples showed focal intranuclear positive reaction with p53 in contrast to negative reaction with an antibody against S100. The patient`s history was discussed at tumor board session. Start of therapy with denosumab was considered the best therapy approach in this calcitrant case.

As far as correspondence reached, denosumab injections were given for almost 3 years (35 months). Unfortunately, success of therapy was not ascertainable.

3.3.6 Patient 6

In August 2016, a 61-year-old man presented with back pain for 4 and a half years and sensomotoric disorders (parasthesia was described at the lateral left thigh). MRI of the vertebral column showed pathological enhancement of contrast medium at L2, decrease in height of the vertebra as well as foraminal stenosis (root of L2). CT scans indicated osteolysis at L2 and stenosis of the left recessus lateralis L2 / L3. PET-CT also showed high storage at the suspicious lesion and no further FTG storing lesion. No problems concerning urinary or fecal incontinence were described. Supplied with two crutches and a back splint, the patient was unable to walk more than a few meters due to intense symptoms.

First medical contact took place in Klagenfurt, histology of incisional biopsy was sent to Vienna as well as to Graz. Histopathological evaluation was consent with GCT. Tumor board in Graz decided on neoadjuvant therapy with denosumab for 3 months. After 2 months, current radiography showed beginning calcification at the margins of the osteolytic process as well as no further progression in loss of height of the vertebra. Clinical presentation of the patient did also improve, sensomotoric disorders were not apparent any more.

The first operation consisted of corporectomy using a ventral approach as well as implantation of a cage to regain dorsal stabilization of the vertebral column (dorsal approach). Due to intraoperative high demand of blood products (12 EC´s, 5g Hämocomplettan, 3000IE Prothromplex, 2TC`s), the patient stayed at intensive care unit for 2 days for observation. However, weaning took place one day after the operation and further post-operative recovery went well beside a brief depressive period.

Two months after the first operation, second took place due to instability and tilting of the artificial bone material. Revision, removal of metals and reimplantation of replacement according to a compound osteosynthesis were performed. The operation went uneventful, as did post-operative recovery. Clinical features improved significantly. The patient was able to walk well, although he further needed crutches, and initially described pain diminished after multiple rehabilitation stays.

On the last follow-up, which was one and a half years after the second operation, no local recurrence or other event became apparent. In this case, denosumab led after only 2 months to ossification of the tumor and enabled surgical therapy in a difficult anatomical location. Again, no side effects were reported.

3.3.7 Patient 7

In February 2007, this 31-year-old man presented with pain at the knee followed by pathological fracture of the femur. First operation took place in Zagreb, including resection of the distal femur and reconstruction with tumor endoprosthesis HMRS. Histology of the removed mass was consent with GCT. Further, multiple soft tissue nodules were removed.

Almost 2 and a half years later, the patient presented at the *Department of Orthopaedics and Trauma* in Graz to obtain a second opinion. Because of the wide extension of local recurrence, which affected approximately the lower half of the left femur, medical professionals in Zagreb recommended the amputation of the leg as soon as possible. A distinct swelling of the left upper leg was apparent in physical examination. Radiography and histological specimen were conveyed at Graz. Local recurrence measured 8.5 x 5.2 x 14.2 cm and was mostly located in soft tissue dorsal at the distal half of the femur, very close to the arteria and vena femuralis superficialis and the nervus tibialis. CT of the thorax showed an impressive finding of multiple lung metastases, the biggest measuring 8 cm in diameter. Lung metastases were adjoining the aorta and the oesophagus and affected both lungs. Enhancement of contrast medium was intermediate high. Another metastasis measured 4 cm and was located near the pericardium in the lingula of the left upper lobe. Multiple lymph nodes were enlarged.

Participation in the *Safety Study of Denosumab in Subjects With Recurrent or Unresectable Giant Cell Tumor of Bone* was evaluated and therapy with denosumab was initiated, 120 mg denosumab s.c. every 4 weeks led to at first slight decrease in size of the lung metastases and after a few months to extensive narrowing of the soft tissue mass in the femur. Halt in progression and distinct calcification of the lesions have been achieved. Denosumab injections were continuously administered until the last follow-up, which took place one and a half

years after start of therapy with denosumab. Due to lack of progression of the lung metastases as well as ossification of the tumor in the femur, no surgical therapy was realized. The patient tolerated therapy with denosumab well and declared to be content with the actual clinical outcome. No side effects were reported.

In total, this patient underwent therapy with denosumab for at least 18 months, and response was satisfying. Compared to the alternative outcome of amputation, denosumab improved therapeutic options immensely for this young man. The recommendation of this patient influenced *Patient 8* to obtain a second opinion of the orthopaedic outpatient clinic in Graz.

3.3.8 Patient 8

In 2010, a 31-year-old woman underwent biopsy and intralesional resection of GCT located at the distal tibia in Zagreb. Adjuvant local radiotherapy was performed and the ankle was immobilized using a plaster cast. Six months after the operation, the patient obtained a second opinion of the *Department of Orthopaedics and Trauma* in Graz. Radiography indicated remaining tumor mass adjoining the distal tibia-fibular joint. Participation in the international study with centrum in Bad Saarau (open-labeled phase 2 study of denosumab) was evaluated and initiated. Subcutaneous injections of 120 mg denosumab every 4 weeks (including loading doses of 120 mg denosumab on day 8 and 15) were administered. Fracture due to radiotherapy occurred.

In 2012, the patient presented again in order to reevaluate surgical therapy in Graz. X-ray showed no further progression in size of the tumor. Half a year later, second operation took place and consisted of curettage, filling with cancellous bone of the iliac crest, reconstruction with allograft and compound osteosynthesis as well as arthrodesis of the left upper ankle joint. The operation went well. Denosumab injections were continuously administered, according to study protocol.

Clinically, the patient was able to walk with crutches. However, she described pain after a longer walk, making breaks necessary. Local hyperpigmentation of the irradiated region was shown. A side effect of therapy with denosumab was reported: The patient developed a calcified soft tissue expansion measuring 5 x 4 x 3 cm at the distal forearm. The lesion occurred where denosumab injections were administered and was surgically removed. Systemic therapy lasted at least 30 months.

More than 2 years after the second operation, the patient again obtained a second opinion. She complained about pain in the past 3 months, swelling under high load and a new feeling of instability at the ankle. Radiography showed breakage of osteosynthesis material. Diverse therapy approaches were proposed to her. Conservative therapy would consist of shoe orthosis. Surgical therapy would include arthrodesis of the upper and the lower ankle joint after removal of metal.

The patient decided to undergo therapy in Zagreb. Unfortunately, no details of therapy are documented. Therefore, date of last follow-up was the day she obtained a second opinion at Graz.

3.3.9 Patient 9

In August 2011, a 49-year-old woman presented with pain and swelling at the right ankle for 4 weeks. X-ray and MRI scans showed a 3 x 3.2 x 3.7 cm measuring partly extraosseous located lesion at the distal tibia. Incisional biopsy was consistent with GCT, first operation followed (curettage and filling with palacos). Additionally, CT of the thorax showed several small lesions of unknown dignity. Concerning the potential lung metastases, observation was decided.

Seven months later, first local recurrence became apparent. MRI scans showed a 1.3 x 1.5 x 1.6 cm big osteolytic lesion adjoining the filling material. Lesions in the lung were unaltered. Second operation consisted of re-curettage and again filling with cement. Post-operative recovery was not as satisfactory as after the first operation, the patient continuously complained about pain, could not walk without crutches and multiple infiltrations did not improve clinical features significantly.

However, lung nodules throughout stayed the same size and therefore were declared as post-inflammatory granuloma.

The third operation took place 17 months after the second because of massive pain. Symptoms were resistant to diverse therapy approaches including physical therapy, administration of local pain-relieving ointments and infiltrations. Additionally, MRI scans showed a small suspicious lesion, which measured only 8 mm in diameter and did not increase in size but was located at the maximum of pain. Re-curettage and filling with cement took place. Histology of the removed mass was consistent with local recurrence of GCT. Unfortunately, symptoms did not diminish. A decent swelling at the right ankle, hyp- and paresthesia as well as electrifying pain were still described. The patient obtained a second opinion of *The Vienna General Hospital (AKH)*. Start of therapy with denosumab (120 mg every 4 weeks for 3 months) was decided in order to reduce the risk of local recurrence and to stabilize bone structure of the multiple operated painful region. Symptoms were still described after therapy with denosumab, mostly occurring under high load.

Date of orthopaedic last follow-up was 5.5 years after end of therapy with denosumab. No side effects were described. However, significant reduction of symptoms was not described either. The patient suffered from different levels of pain over a time period of 7 years and continuously needed a crutch or other medical tool to walk.

3.3.10 Overview

The overall therapy duration lasted on average 14.6 months. Six patients received denosumab for ≥ 10 months.

Table 2 shows epidemiologic data, location of GCT, appearance of local recurrence and metastases as well as duration and number of therapies with denosumab. Further, details regarding pain levels under therapy are listed. Data on radiological response to denosumab (calcification and reduction in size of lesions), improvement of surgical therapy, side effects of denosumab and most invasive surgical therapy in the end are shown in ***Table 3***.

Characteristics		LR	Metastases	Therapy duration	Pain under denosumab therapy
Patient 1	Female 52 years Humerus	3	none	3 times, in total 15 months	persisting pain
Patient 2	Male 27 years Femur	1	unclear lesions	14 months	no pain declared
Patient 3	Male 21 years Humerus	2	none	3 months	no pain declared
Patient 4	Female 32 years Radius (multifocal)	3	none	2 times, in total 10 months	no pain declared
Patient 5	Male 55 years Tibia	2	lung metastases	35 months	NA
Patient 6	Male 61 years L2	0	none	3 months	decrease in pain
Patient 7	Male 31 years Femur	> 1	lung metastases	18 months	no pain declared
Patient 8	Female 31 years Tibia	0	none	> 30 months	persisting pain
Patient 9	Female 49 years Tibia	2	none	3 months	persisting pain

Table 2

Characteristics of patients treated with denosumab. LR means local recurrence. Every LR was counted in this table, not only those after therapy with denosumab.

	Calcification	Reduction in size	Improvement of surgical therapy	Side effects	Surgical therapy
1	yes	stable size	yes	none	endoprosthesis
2	yes	stable size	yes	none	endoprosthesis
3	yes	stable size	yes	none	endoprosthesis
4	NA	yes	yes	none	arthrodesis
5	NA	NA	NA	NA	NA
6	yes	stable size	yes	none	compound osteosynthesis
7	yes	yes	operation not necessary any more	none	none / no amputation
8	yes	stable size	yes	calcified soft tissue expansion	arthrodesis
9	NA	NA	none	none	curettage

Table 3 *Therapeutical response to denosumab.*
Increase in size was in no case observed. Information that could not be ascertained is marked with NA (not available). Procedures listed under surgical therapy resemble the operation of highest morbidity of each patient.

Use of denosumab led to improvement of surgical therapy in 6 patients due to downsizing of lesions (Patient 4) and calcification (Patient 1, 2, 3, 6, 8). Better defined boundaries of lesions were seen in every case of calcification and therefore facilitated operations. Considering Patient 7, denosumab rendered surgical therapy completely redundant and prevented amputation.

4. Discussion

GCTs are rare intermediate bone tumors and most patients are sufficiently treated with surgical therapy. However, surgery can be followed by high morbidity in some cases, which is especially inimical when taking the young age of patients into account. In addition, a loss of mobility for the rest of the life with all negative effects on social and work life can occur. This is why research on alternative therapy options, resulting in less invasive operations, is of great importance.

4.1 Verification of diagnoses

Diagnosing GCT lesions can be difficult in cases of untypical anatomical location and/or untypical histological and radiological appearances. Differentiation between primary ABC and cystic GCT (with secondary ABC) had been especially difficult in the past. Specimen had therefore been sent to pathologists in Berlin/Germany or Miami/New York/USA to obtain a second opinion. Interestingly, diagnoses on the same histological samples were quite diverse, ranging from “highly malignant giant cell-rich osteosarcoma” to “benign giant cell tumor of bone with secondary ABC”. This example highlights the importance of new diagnostic methods and the antibody against H3.3 G34W, which stains for the most common mutation in GCTs. Diagnoses of all patients included into this retrospective analysis were verified either by histological or immunohistochemical methods or by mutational analyses. This ensured that only patients that truly were affected by GCT were enclosed in this statistical analysis.

4.2 Patient characteristics

As previous studies showed, a slight predominance of women could be seen in our cohort of patients (48.1% (n=26) were male, 51.9% (n=28) were female). The 95% confidence interval for age at diagnosis was 33.6 – 42.2 years which also resembles findings of other studies. (2) Of note, there indeed were outliers in our cohort (5 patients were older than 60 years, 6 patients were younger than 20 years).

Regarding patient`s history prior to admission, the vast majority (78.6%) experienced symptoms for ≤ 6 months and pain was by far (86.5%) the most common complain as well as the major reason for admission (73.2%). One might argue that 54 patients compromise only a small cohort, but considering the rareness of GCT and the fact, that solely patients with verifiable diagnoses were enrolled, the number of patients reflect targeted study quality.

4.3 Tumor specifications

Up to date, no reports about a favored body side can be found in literature. However, 59.3% of the tumors in our cohort were located at the left side, whilst only 38.9% were found at the right side. Also, GCTs are described as lesions with a typical range from 5 to 15 cm, in contrast to our findings where 63% measured less than 5 cm. (49) The most common location of GCT was around the knee joint (n=30, 55.6%), followed by the distal radius and the wrist joint (n=7, 13%). The biggest GCT lesions were all found at the distal femur.

Multifocal lesions were observed in one patient (1.9%) who also received denosumab therapy (Patient 4). The lesions affected the distal radius, the os lunatum, the os scaphoideum as well as the os capitatum. Two patients (3.7%) developed lung metastases. Of note, only lung nodules that were confirmed by biopsy as metastases of GCT were counted. According to literature, multifocal lesions constitute 1% of GCTs and usually affect hands and feet. Details on lung metastases rates vary depending on study design and literature, ranging from 1-2% of patients (49) or 3% of patients treated with denosumab (103) up to 3 – 7% of all GCT patients. (4) Therefore, our findings regarding frequency of multifocal lesions and metastases approximately resemble the actual state of knowledge.

4.4 Therapy

Overall, every patient underwent at least one operation. Most patients (59.3%) were treated with a single surgery. The maximum of operations performed was 6 times. One patient underwent this high number of operations due to repeated aseptic loosening of screws. Three changes of knee endoprostheses were necessary, as well as mobilization in narcosis due to distinct flexion deficit (E/F: 0/0/50). Neoadjuvant therapies consisted of denosumab or zoledronic acid. Adjuvant therapies included denosumab in most cases (80% of adjuvant treatments) and radiotherapy as well as zoledronic acid.

Almost three quarter of patients (74.1%) were not affected by local recurrence at any time. Most patients that developed recurrence did so for only one time. No statistically significant correlation between local recurrence and size of primary lesion was found (p=0.904). Of note, intervals between surgical removal and local recurrences shortened with number of relapses (mean time prior to first recurrence: 46.4 months, prior to second recurrence: 25.9 months, prior to third recurrence: 6.5 months). Re-operation was the most common therapy of local recurrence (53.8%), followed by use of denosumab (in total 46.2%, denosumab alone was used in 7.7% of all cases of recurrence). These findings show that the majority of patients is satisfactorily treated with surgical therapy, but there is also a number of cases suffering from multiple operations (40.7%) and recurrences (25.9%) that cannot be overlooked.

4.5 Therapy with denosumab

Most patients are optimally treated by surgical therapy alone. However, in case of recurrent and recalcitrant GCT, previous therapy options were unsatisfying and led to operations with high morbidity and poor outcome. Through systemic use of denosumab, calcification of lesions can be achieved, resulting in less invasive operations. Rapid calcification took place in five patients (Patient 1, 3, 6, 7, 8) and further in one patient after prolonged therapy duration (Patient 2). It has to be highlighted, that in every patient where radiological response to denosumab was evaluated, calcification took place. Further progression of disease was observed in no case, shrinkage in size of the lesions happened in two cases (Patient 4, 7).

Improvement of surgical therapy took place in six patients. Better defined margins due to calcification facilitated operations. Further, denosumab-induced downsizing of lesions reduced morbidity of operations. Surgical therapy was not necessary any more in one case of wide local recurrence where amputation of the leg could be prevented through use of denosumab (Patient 7).

Previous studies indicated no influence of denosumab on metastasis rate, although it is hard to statistically prove this statement because of the low number of patients with GCT generally affected by metastases. (127) Statements about the influence on local recurrence rates vary. However, post-operative use of denosumab does not seem to increase recurrence rates. (103, 104) In our cohort, lung metastases were confirmed by biopsy in two cases (Patient 5, 7) and significant reduction in size of metastases under denosumab took place in one case (in the other case, no information was ascertainable). Local recurrence after therapy with denosumab affected two patients (Patient 1, 4). Definition of clinical response to denosumab varies, however, reduction in pain and improvement in mobility are most commonly considered as good response. (99) In our study, only one patient (Patient 6) described decrease in pain, whereas three patients (Patient 1, 8, 9) further complained pain at night, under higher load or even the whole day. Improved mobility took place in three cases (Patient 6 was able to walk again; Patient 7: no amputation; Patient 8: as far as ascertainable, only arthrodesis of the upper ankle joint, compared to arthrodesis of both ankle joints). Therefore, three patients showed distinct clinical benefit.

A possible adverse event was described in one patient (Patient 8). A calcified soft tissue expansion developed where denosumab injections were given. To my knowledge, this side effect had never before been reported in literature, and doctor`s letters indicate planned publication of this case. However, histological specimens never seemed to be sent from Zagreb, where the suspicious lesion was removed, to Graz, so no evidence could be raised to confirm this adverse event. The patient received denosumab injections for at least 30 months and was included in the open-labeled phase 2 study of denosumab, which also did not report about a treatment-related side effect like this. (99) If this adverse event proofed to happen more often, varying locations of injections might help to prevent it.

According to literature, the most common complications of denosumab are known to be nausea, bone pain, headache and fatigue, affecting 18-25% of patients. (99, 100, 107) Incidences of osteonecrosis of the jaw (ONJ) are reported to be up to 6%, this severe complication seems to be dependent on the status of teeth before treatment as well as on the applicated dosis of denosumab injections. (97) Therefore, dental clarification took place before therapy start, so only patients with discreet dental status underwent therapy in the first place. Hypocalcaemia and malignant transformation were in no case observed, neither were further side effects.

On the one side, denosumab is helpful and effective to improve surgical therapy and therefore also outcome of the patients. Better mobility and even preservation of an extremity could be reached through denosumab. On the other side, no reduction of pain was evident in three cases of intense symptoms. Regarding safety of denosumab, no concerns derived from our analysis. Overall, six patients (Patient 1, 2, 4, 5, 7, 8) in our study received denosumab for ≥ 10 months and four (Patient 2, 5, 7, 8) can be considered as long-term denosumab patients (continuous administration of denosumab for 14 up to 35 months). With the exception of one described adverse event (soft tissue expansion), which retrospectively cannot be confirmed as treatment related, no side effects were observed.

4.6 Limitations

One limitation of this retrospective analysis is lack of information due to varying treatment places. The *Department of Orthopedics and Trauma, Medical University of Graz* is not only a national center of expertise for bone tumors but also has a profound reputation in our adjoining countries. In addition, GCT lesions are rare, favoring the obtaining of a second opinion, and studies with new therapy approaches like denosumab are often multi-centered. Therefore, some information could not be ascertained. Due to the retrospective design of this study, collected data depended on comprehensiveness of doctor`s letters. Patient`s history (time and quality of symptoms, reasons for admission…) for example was not always documented and hence could not be analyzed in every case.

4.7 Closing statement

The chronological order of *suspected diagnosis of GCT – either verification of diagnosis through biopsy or through intra-surgical frozen section analysis – definite operation – no signs of local recurrence and no further symptoms in follow-up* demonstrates the best possible therapeutic outcome. Considering patients in whom diagnosis of GCT is difficult, new scientific achievements (immunohistochemical staining with an antibody directed against H3.3 G34W) facilitate easier confirmation of diagnosis. Regarding patients with GCT in unresectable cases, due to width of extension for example, long-time therapy with denosumab constitutes a good and safe therapy option. In GCT where surgical therapy would be inappropriate and presumably come along with high morbidity and movement restriction due to difficult anatomical locations, neoadjuvant therapy with denosumab is helpful and effective.

GCTs do not show high mortality rates. Not a single patient from our cohort died. However, this should not demotivate spirit of research, because there are still unanswered questions to explore. First, the risk factors for GCT recurrence are still ununderstood. On the one hand, studies state that biological behavior and type of performed surgery are the most important risk factors. (103) On the other hand, reports of increased local recurrence rates after pre-operative use of denosumab exist. (104) Second, there is still no standardized therapy schema for patients with unresectable GCT under denosumab therapy. How long should injections be given? Lifelong? Does reduction of dose resemble an option, or are longer intervals between injections possible? Third, further questions arise with long therapy duration. Considering the young age of patients and the slight predominance of women, pregnancy will sooner or later be an issue for patients. How long should denosumab injections be paused for pregnancy and nursing? Lastly, it is still unknown how to predict which patients are at risk to develop lung metastases.

4.8 Key facts about denosumab in GCT patients

1. Clinical benefits varied. Denosumab increased mobility of the patients, whilst reduction of pain did not take place in 3 cases with intense symptoms.

2. Radiological response was distinct. Calcification was seen in every case radiologically evaluated. Halt in progression could be achieved through denosumab, downsizing of GCT affected 2 cases.

3. Histological response was characterized by depletion of giant cells and formation of new bone. Neoplastic stromal cells survived denosumab therapy.

4. Surgical therapy was significantly improved or rendered useless in 7 cases. Better defined margins of lesions facilitated operations.

5. Regarding safety of denosumab, no concerns regarding usage derived from our retrospective case study.

References

1. WHO Classification of Tumours: Soft Tissue and Bone Tumours. 5 ed. Lyon, France: Internation Agency for Research on Cancer; 2020.
2. Raskin KA, Schwab JH, Mankin HJ, Springfield DS, Hornicek FJ. Giant cell tumor of bone. J Am Acad Orthop Surg. 2013;21(2):118-26.
3. Jaffe HL, Lichtenstein L, Portis RB. Giant cell tumor of bone: its pathological appearance, grading, supposed variants and treatment. Arch Pathol. 1940:993-1031.
4. Flanagan AM, Larousserie F, O`Donnell PG, et.al. Giant cell tumour of bone. In: WHO Classification of Tumours Editorial Bourd, ed *WHO Classification of Tumours: Soft Tissue and Bone Tumours, Volume 3*. 5th ed. Lyon, France: International Agency for Research on Cancer; 2020. p. 440-6.
5. Niu X, Zhang Q, Hao L, Ding Y, Li Y, Xu H, et al. Giant cell tumor of the extremity: retrospective analysis of 621 Chinese patients from one institution. J Bone Joint Surg Am. 2012;94(5):461-7.
6. Rockberg J, Bach BA, Amelio J, Hernandez RK, Sobocki P, Engellau J, et al. Incidence Trends in the Diagnosis of Giant Cell Tumor of Bone in Sweden Since 1958. J Bone Joint Surg Am. 2015;97(21):1756-66.
7. Liede A, Bach BA, Stryker S, Hernandez RK, Sobocki P, Bennett B, et al. Regional variation and challenges in estimating the incidence of giant cell tumor of bone. J Bone Joint Surg Am. 2014;96(23):1999-2007.
8. Coley B. Giant cell tumor (osteoclastoma). In: Hoeber, editor. Neoplasms of Bone and Related Conditions. 2 ed. New York1960. p. 196-235.
9. Wang T, Jiao J, Zhang H, Zhou W, Li Z, Han S, et al. TGF-β induced PAR-1 expression promotes tumor progression and osteoclast differentiation in giant cell tumor of bone. Int J Cancer. 2017;141(8):1630-42.
10. Matsubayashi S, Nakashima M, Kumagai K, Egashira M, Naruke Y, Kondo H, et al. Immunohistochemical analyses of beta-catenin and cyclin D1 expression in giant cell tumor of bone (GCTB): a possible role of Wnt pathway in GCTB tumorigenesis. Pathol Res Pract. 2009;205(9):626-33.
11. Kauzman A, Li SQ, Bradley G, Bell RS, Wunder JS, Kandel R. Cyclin alterations in giant cell tumor of bone. Mod Pathol. 2003;16(3):210-8.
12. Okubo T, Saito T, Mitomi H, Takagi T, Torigoe T, Suehara Y, et al. p53 mutations may be involved in malignant transformation of giant cell tumor of bone through interaction with GPX1. Virchows Arch. 2013;463(1):67-77.
13. Saâda E, Peoc'h M, Decouvelaere AV, Collard O, Peyron AC, Pedeutour F. CCND1 and MET genomic amplification during malignant transformation of a giant cell tumor of bone. J Clin Oncol. 2011;29(4):e86-9.
14. Li Z, Jiao X, Di Sante G, Ertel A, Casimiro MC, Wang M, et al. Cyclin D1 integrates G9a-mediated histone methylation. Oncogene. 2019;38(22):4232-49.
15. Kandel R, Li SQ, Bell R, Wunder J, Ferguson P, Kauzman A, et al. Cyclin D1 and p21 is elevated in the giant cells of giant cell tumors. J Orthop Res. 2006;24(3):428-37.
16. van Dam H, Castellazzi M. Distinct roles of Jun : Fos and Jun : ATF dimers in oncogenesis. Oncogene. 2001;20(19):2453-64.
17. Noh BJ, Park YK. Giant cell tumor of bone: updated molecular pathogenesis and tumor biology. Hum Pathol. 2018;81:1-8.

18. Wu M, Chen G, Li YP. TGF-β and BMP signaling in osteoblast, skeletal development, and bone formation, homeostasis and disease. Bone Res. 2016;4:16009.
19. Pratap J, Galindo M, Zaidi SK, Vradii D, Bhat BM, Robinson JA, et al. Cell growth regulatory role of Runx2 during proliferative expansion of preosteoblasts. Cancer Res. 2003;63(17):5357-62.
20. Lee JS, Thomas DM, Gutierrez G, Carty SA, Yanagawa S, Hinds PW. HES1 cooperates with pRb to activate RUNX2-dependent transcription. J Bone Miner Res. 2006;21(6):921-33.
21. Singh S, Mak IW, Cowan RW, Turcotte R, Singh G, Ghert M. The role of TWIST as a regulator in giant cell tumor of bone. J Cell Biochem. 2011;112(9):2287-95.
22. Singh S, Singh M, Mak IW, Turcotte R, Ghert M. Investigation of FGFR2-IIIC signaling via FGF-2 ligand for advancing GCT stromal cell differentiation. PLoS One. 2012;7(10):e46769.
23. Zheng MH, Fan Y, Smith A, Wysocki S, Papadimitriou JM, Wood DJ. Gene expression of monocyte chemoattractant protein-1 in giant cell tumors of bone osteoclastoma: possible involvement in CD68+ macrophage-like cell migration. J Cell Biochem. 1998;70(1):121-9.
24. Yu Q, Stamenkovic I. Cell surface-localized matrix metalloproteinase-9 proteolytically activates TGF-beta and promotes tumor invasion and angiogenesis. Genes Dev. 2000;14(2):163-76.
25. Branstetter DG, Nelson SD, Manivel JC, Blay JY, Chawla S, Thomas DM, et al. Denosumab induces tumor reduction and bone formation in patients with giant-cell tumor of bone. Clin Cancer Res. 2012;18(16):4415-24.
26. Dougall WC, Glaccum M, Charrier K, Rohrbach K, Brasel K, De Smedt T, et al. RANK is essential for osteoclast and lymph node development. Genes Dev. 1999;13(18):2412-24.
27. Atkins GJ, Kostakis P, Vincent C, Farrugia AN, Houchins JP, Findlay DM, et al. RANK Expression as a cell surface marker of human osteoclast precursors in peripheral blood, bone marrow, and giant cell tumors of bone. J Bone Miner Res. 2006;21(9):1339-49.
28. Wada T, Nakashima T, Hiroshi N, Penninger JM. RANKL-RANK signaling in osteoclastogenesis and bone disease. Trends Mol Med. 2006;12(1):17-25.
29. Skubitz KM. Giant cell tumor of bone: current treatment options. Curr Treat Options Oncol. 2014;15(3):507-18.
30. Matsuo K, Irie N. Osteoclast-osteoblast communication. Arch Biochem Biophys. 2008;473(2):201-9.
31. Negishi-Koga T, Shinohara M, Komatsu N, Bito H, Kodama T, Friedel RH, et al. Suppression of bone formation by osteoclastic expression of semaphorin 4D. Nat Med. 2011;17(11):1473-80.
32. Kato I, Furuya M, Matsuo K, Kawabata Y, Tanaka R, Ohashi K. Giant cell tumours of bone treated with denosumab: histological, immunohistochemical and H3F3A mutation analyses. Histopathology. 2018;72(6):914-22.
33. Kim MH, Park M, Baek SH, Kim HJ, Kim SH. Molecules and signaling pathways involved in the expression of OC-STAMP during osteoclastogenesis. Amino Acids. 2011;40(5):1447-59.
34. Gohda J, Akiyama T, Koga T, Takayanagi H, Tanaka S, Inoue J. RANK-mediated amplification of TRAF6 signaling leads to NFATc1 induction during osteoclastogenesis. Embo j. 2005;24(4):790-9.

35. Pilkington MF, Sims SM, Dixon SJ. Transforming growth factor-beta induces osteoclast ruffling and chemotaxis: potential role in osteoclast recruitment. J Bone Miner Res. 2001;16(7):1237-47.
36. Ek-Rylander B, Flores M, Wendel M, Heinegård D, Andersson G. Dephosphorylation of osteopontin and bone sialoprotein by osteoclastic tartrate-resistant acid phosphatase. Modulation of osteoclast adhesion in vitro. J Biol Chem. 1994;269(21):14853-6.
37. Cowan RW, Ghert M, Singh G. T cells stimulate catabolic gene expression by the stromal cells from giant cell tumor of bone. Biochem Biophys Res Commun. 2012;419(4):719-23.
38. Mak IW, Turcotte RE, Ghert M. Parathyroid hormone-related protein (PTHrP) modulates adhesion, migration and invasion in bone tumor cells. Bone. 2013;55(1):198-207.
39. Klein GL, Castro SM, Garofalo RP. The calcium-sensing receptor as a mediator of inflammation. Semin Cell Dev Biol. 2016;49:52-6.
40. Ng PK, Tsui SK, Lau CP, Wong CH, Wong WH, Huang L, et al. CCAAT/enhancer binding protein beta is up-regulated in giant cell tumor of bone and regulates RANKL expression. J Cell Biochem. 2010;110(2):438-46.
41. Lum L, Wong BR, Josien R, Becherer JD, Erdjument-Bromage H, Schlöndorff J, et al. Evidence for a role of a tumor necrosis factor-alpha (TNF-alpha)-converting enzyme-like protease in shedding of TRANCE, a TNF family member involved in osteoclastogenesis and dendritic cell survival. J Biol Chem. 1999;274(19):13613-8.
42. Lindroth AM, Plass C. Recurrent H3.3 alterations in childhood tumors. Nat Genet. 2013;45(12):1413-4.
43. Schwartzentruber J, Korshunov A, Liu XY, Jones DT, Pfaff E, Jacob K, et al. Driver mutations in histone H3.3 and chromatin remodelling genes in paediatric glioblastoma. Nature. 2012;482(7384):226-31.
44. Behjati S, Tarpey PS, Presneau N, Scheipl S, Pillay N, Van Loo P, et al. Distinct H3F3A and H3F3B driver mutations define chondroblastoma and giant cell tumor of bone. Nat Genet. 2013;45(12):1479-82.
45. Kervarrec T, Collin C, Larousserie F, Bouvier C, Aubert S, Gomez-Brouchet A, et al. H3F3 mutation status of giant cell tumors of the bone, chondroblastomas and their mimics: a combined high resolution melting and pyrosequencing approach. Mod Pathol. 2017;30(3):393-406.
46. Presneau N, Baumhoer D, Behjati S, Pillay N, Tarpey P, Campbell PJ, et al. Diagnostic value of H3F3A mutations in giant cell tumour of bone compared to osteoclast-rich mimics. J Pathol Clin Res. 2015;1(2):113-23.
47. Cleven AH, Höcker S, Briaire-de Bruijn I, Szuhai K, Cleton-Jansen AM, Bovée JV. Mutation Analysis of H3F3A and H3F3B as a Diagnostic Tool for Giant Cell Tumor of Bone and Chondroblastoma. Am J Surg Pathol. 2015;39(11):1576-83.
48. Yamamoto H, Iwasaki T, Yamada Y, Matsumoto Y, Otsuka H, Yoshimoto M, et al. Diagnostic utility of histone H3.3 G34W, G34R, and G34V mutant-specific antibodies for giant cell tumors of bone. Hum Pathol. 2018;73:41-50.
49. Nielsen ARG. Diagnostic Pathology: Bone. 2 ed. Salt Lake City, UT: Elsevier, Inc.; 2017. 480 p.
50. Morgan T, Atkins GJ, Trivett MK, Johnson SA, Kansara M, Schlicht SL, et al. Molecular profiling of giant cell tumor of bone and the osteoclastic localization

of ligand for receptor activator of nuclear factor kappaB. Am J Pathol. 2005;167(1):117-28.
51. Bertoni F, Bacchini P, Staals EL. Malignancy in giant cell tumor of bone. Cancer. 2003;97(10):2520-9.
52. Amary F, Berisha F, Ye H, Gupta M, Gutteridge A, Baumhoer D, et al. H3F3A (Histone 3.3) G34W Immunohistochemistry: A Reliable Marker Defining Benign and Malignant Giant Cell Tumor of Bone. Am J Surg Pathol. 2017;41(8):1059-68.
53. Gong L, Liu W, Sun X, Sajdik C, Tian X, Niu X, et al. Histological and clinical characteristics of malignant giant cell tumor of bone. Virchows Arch. 2012;460(3):327-34.
54. Martin C, McCarthy EF. Giant cell tumor of the sacrum and spine: series of 23 cases and a review of the literature. Iowa Orthop J. 2010;30:69-75.
55. Sanjay BK, Sim FH, Unni KK, McLeod RA, Klassen RA. Giant-cell tumours of the spine. J Bone Joint Surg Br. 1993;75(1):148-54.
56. Oliveira VC, van der Heijden L, van der Geest IC, Campanacci DA, Gibbons CL, van de Sande MA, et al. Giant cell tumours of the small bones of the hands and feet: long-term results of 30 patients and a systematic literature review. Bone Joint J. 2013;95-b(6):838-45.
57. Amary F, Markert E, Berisha F, Ye H, Gerrand C, Cool P, et al. FOS Expression in Osteoid Osteoma and Osteoblastoma: A Valuable Ancillary Diagnostic Tool. Am J Surg Pathol. 2019;43(12):1661-7.
58. Eckardt JJ, Grogan TJ. Giant cell tumor of bone. Clin Orthop Relat Res. 1986(204):45-58.
59. Turcotte RE. Giant cell tumor of bone. Orthop Clin North Am. 2006;37(1):35-51.
60. Campanacci M, Baldini N, Boriani S, Sudanese A. Giant-cell tumor of bone. J Bone Joint Surg Am. 1987;69(1):106-14.
61. Bertoni F, Present D, Enneking WF. Giant-cell tumor of bone with pulmonary metastases. J Bone Joint Surg Am. 1985;67(6):890-900.
62. Chen CC, Liau CT, Chang CH, Hsu YH, Shih HN. Giant Cell Tumors of the Bone With Pulmonary Metastasis. Orthopedics. 2016;39(1):e68-73.
63. Chakarun CJ, Forrester DM, Gottsegen CJ, Patel DB, White EA, Matcuk GR, Jr. Giant cell tumor of bone: review, mimics, and new developments in treatment. Radiographics. 2013;33(1):197-211.
64. Murphey MD, Nomikos GC, Flemming DJ, Gannon FH, Temple HT, Kransdorf MJ. From the archives of AFIP. Imaging of giant cell tumor and giant cell reparative granuloma of bone: radiologic-pathologic correlation. Radiographics. 2001;21(5):1283-309.
65. Aoki J, Tanikawa H, Ishii K, Seo GS, Karakida O, Sone S, et al. MR findings indicative of hemosiderin in giant-cell tumor of bone: frequency, cause, and diagnostic significance. AJR Am J Roentgenol. 1996;166(1):145-8.
66. Verstraete KL, Lang P. Bone and soft tissue tumors: the role of contrast agents for MR imaging. Eur J Radiol. 2000;34(3):229-46.
67. van der Heijden L, Dijkstra PDS, Blay JY, Gelderblom H. Giant cell tumour of bone in the denosumab era. Eur J Cancer. 2017;77:75-83.
68. Deheshi BM, Jaffer SN, Griffin AM, Ferguson PC, Bell RS, Wunder JS. Joint salvage for pathologic fracture of giant cell tumor of the lower extremity. Clin Orthop Relat Res. 2007;459:96-104.

69. Takeda N, Kobayashi T, Tandai S, Matsuno T, Shirado O, Watanabe T, et al. Treatment of giant cell tumors in the sacrum and spine with curettage and argon beam coagulator. J Orthop Sci. 2009;14(2):210-4.
70. Lin WH, Lan TY, Chen CY, Wu K, Yang RS. Similar local control between phenol- and ethanol-treated giant cell tumors of bone. Clin Orthop Relat Res. 2011;469(11):3200-8.
71. Gortzak Y, Kandel R, Deheshi B, Werier J, Turcotte RE, Ferguson PC, et al. The efficacy of chemical adjuvants on giant-cell tumour of bone. An in vitro study. J Bone Joint Surg Br. 2010;92(10):1475-9.
72. Algawahmed H, Turcotte R, Farrokhyar F, Ghert M. High-Speed Burring with and without the Use of Surgical Adjuvants in the Intralesional Management of Giant Cell Tumor of Bone: A Systematic Review and Meta-Analysis. Sarcoma. 2010;2010.
73. Blackley HR, Wunder JS, Davis AM, White LM, Kandel R, Bell RS. Treatment of giant-cell tumors of long bones with curettage and bone-grafting. J Bone Joint Surg Am. 1999;81(6):811-20.
74. Boons HW, Keijser LC, Schreuder HW, Pruszczynski M, Lemmens JA, Veth RP. Oncologic and functional results after treatment of giant cell tumors of bone. Arch Orthop Trauma Surg. 2002;122(1):17-23.
75. Malawer MM, Bickels J, Meller I, Buch RG, Henshaw RM, Kollender Y. Cryosurgery in the treatment of giant cell tumor. A long-term followup study. Clin Orthop Relat Res. 1999(359):176-88.
76. Jacobs PA, Clemency RE, Jr. The closed cryosurgical treatment of giant cell tumor. Clin Orthop Relat Res. 1985(192):149-58.
77. Marcove RC, Weis LD, Vaghaiwalla MR, Pearson R. Cryosurgery in the treatment of giant cell tumors of bone: a report of 52 consecutive cases. Clin Orthop Relat Res. 1978(134):275-89.
78. Mankin HJ, Hornicek FJ. Treatment of giant cell tumors with allograft transplants: a 30-year study. Clin Orthop Relat Res. 2005;439:144-50.
79. Schindler OS, Cannon SR, Briggs TW, Blunn GW. Use of a novel bone graft substitute in peri-articular bone tumours of the knee. Knee. 2007;14(6):458-64.
80. Harms C, Helms K, Taschner T, Stratos I, Ignatius A, Gerber T, et al. Osteogenic capacity of nanocrystalline bone cement in a weight-bearing defect at the ovine tibial metaphysis. Int J Nanomedicine. 2012;7:2883-9.
81. Theler JM. Bone tissue substitutes and replacements. Curr Opin Otolaryngol Head Neck Surg. 2011;19(4):317-22.
82. Ma Y, Xu W, Yin H, Huang Q, Liu T, Yang X, et al. Therapeutic radiotherapy for giant cell tumor of the spine: a systemic review. Eur Spine J. 2015;24(8):1754-60.
83. Bhatia S, Miszczyk L, Roelandts M, Nguyen TD, Boterberg T, Poortmans P, et al. Radiotherapy for marginally resected, unresectable or recurrent giant cell tumor of the bone: a rare cancer network study. Rare Tumors. 2011;3(4):e48.
84. Shi W, Indelicato DJ, Reith J, Smith KB, Morris CG, Scarborough MT, et al. Radiotherapy in the management of giant cell tumor of bone. Am J Clin Oncol. 2013;36(5):505-8.
85. Lau CP, Huang L, Wong KC, Kumta SM. Comparison of the anti-tumor effects of denosumab and zoledronic acid on the neoplastic stromal cells of giant cell tumor of bone. Connect Tissue Res. 2013;54(6):439-49.

86. Ott SM. Sclerostin and Wnt signaling--the pathway to bone strength. J Clin Endocrinol Metab. 2005;90(12):6741-3.
87. Baron R, Rawadi G. Targeting the Wnt/beta-catenin pathway to regulate bone formation in the adult skeleton. Endocrinology. 2007;148(6):2635-43.
88. Gatti D, Viapiana O, Fracassi E, Idolazzi L, Dartizio C, Povino MR, et al. Sclerostin and DKK1 in postmenopausal osteoporosis treated with denosumab. J Bone Miner Res. 2012;27(11):2259-63.
89. Li J, Sarosi I, Yan XQ, Morony S, Capparelli C, Tan HL, et al. RANK is the intrinsic hematopoietic cell surface receptor that controls osteoclastogenesis and regulation of bone mass and calcium metabolism. Proc Natl Acad Sci U S A. 2000;97(4):1566-71.
90. Weinstein RS, Roberson PK, Manolagas SC. Giant osteoclast formation and long-term oral bisphosphonate therapy. N Engl J Med. 2009;360(1):53-62.
91. Gatti D, Viapiana O, Idolazzi L, Fracassi E, Rossini M, Adami S. The waning of teriparatide effect on bone formation markers in postmenopausal osteoporosis is associated with increasing serum levels of DKK1. J Clin Endocrinol Metab. 2011;96(5):1555-9.
92. Chen KH, Wu PK, Chen CF, Chen WM. Zoledronic acid-loaded bone cement as a local adjuvant therapy for giant cell tumor of the sacrum after intralesional curettage. Eur Spine J. 2015;24(10):2182-8.
93. Nishisho T, Hanaoka N, Miyagi R, Sakai T, Toki S, Takahashi M, et al. Local administration of zoledronic acid for giant cell tumor of bone. Orthopedics. 2015;38(1):e25-30.
94. Stopeck AT, Lipton A, Body JJ, Steger GG, Tonkin K, de Boer RH, et al. Denosumab compared with zoledronic acid for the treatment of bone metastases in patients with advanced breast cancer: a randomized, double-blind study. J Clin Oncol. 2010;28(35):5132-9.
95. Henry DH, Costa L, Goldwasser F, Hirsh V, Hungria V, Prausova J, et al. Randomized, double-blind study of denosumab versus zoledronic acid in the treatment of bone metastases in patients with advanced cancer (excluding breast and prostate cancer) or multiple myeloma. J Clin Oncol. 2011;29(9):1125-32.
96. Deveci MA, Paydaş S, Gönlüşen G, Özkan C, Biçer Ö S, Tekin M. Clinical and pathological results of denosumab treatment for giant cell tumors of bone: Prospective study of 14 cases. Acta Orthop Traumatol Turc. 2017;51(1):1-6.
97. Palmerini E, Chawla NS, Ferrari S, Sudan M, Picci P, Marchesi E, et al. Denosumab in advanced/unresectable giant-cell tumour of bone (GCTB): For how long? Eur J Cancer. 2017;76:118-24.
98. Lewiecki EM. Clinical use of denosumab for the treatment for postmenopausal osteoporosis. Curr Med Res Opin. 2010;26(12):2807-12.
99. Thomas D, Henshaw R, Skubitz K, Chawla S, Staddon A, Blay JY, et al. Denosumab in patients with giant-cell tumour of bone: an open-label, phase 2 study. Lancet Oncol. 2010;11(3):275-80.
100. Chawla S, Henshaw R, Seeger L, Choy E, Blay JY, Ferrari S, et al. Safety and efficacy of denosumab for adults and skeletally mature adolescents with giant cell tumour of bone: interim analysis of an open-label, parallel-group, phase 2 study. Lancet Oncol. 2013;14(9):901-8.
101. Goldschlager T, Dea N, Boyd M, Reynolds J, Patel S, Rhines LD, et al. Giant cell tumors of the spine: has denosumab changed the treatment paradigm? J Neurosurg Spine. 2015;22(5):526-33.

102. Mattei TA, Ramos E, Rehman AA, Shaw A, Patel SR, Mendel E. Sustained long-term complete regression of a giant cell tumor of the spine after treatment with denosumab. Spine J. 2014;14(7):e15-21.
103. Luengo-Alonso G, Mellado-Romero M, Shemesh S, Ramos-Pascua L, Pretell-Mazzini J. Denosumab treatment for giant-cell tumor of bone: a systematic review of the literature. Arch Orthop Trauma Surg. 2019;139(10):1339-49.
104. Chen X, Li H, Zhu S, Wang Y, Qian W. Pre-operative denosumab is associated with higher risk of local recurrence in giant cell tumor of bone: a systematic review and meta-analysis. BMC Musculoskelet Disord. 2020;21(1):256.
105. Li H, Gao J, Gao Y, Lin N, Zheng M, Ye Z. Denosumab in Giant Cell Tumor of Bone: Current Status and Pitfalls. Front Oncol. 2020;10:580605.
106. Müller DA, Beltrami G, Scoccianti G, Campanacci DA, Franchi A, Capanna R. Risks and benefits of combining denosumab and surgery in giant cell tumor of bone-a case series. World J Surg Oncol. 2016;14(1):281.
107. Rutkowski P, Ferrari S, Grimer RJ, Stalley PD, Dijkstra SP, Pienkowski A, et al. Surgical downstaging in an open-label phase II trial of denosumab in patients with giant cell tumor of bone. Ann Surg Oncol. 2015;22(9):2860-8.
108. Ueda T, Morioka H, Nishida Y, Kakunaga S, Tsuchiya H, Matsumoto Y, et al. Objective tumor response to denosumab in patients with giant cell tumor of bone: a multicenter phase II trial. Ann Oncol. 2015;26(10):2149-54.
109. Roitman PD, Jauk F, Farfalli GL, Albergo JI, Aponte-Tinao LA. Denosumab-treated giant cell tumor of bone. Its histologic spectrum and potential diagnostic pitfalls. Hum Pathol. 2017;63:89-97.
110. Borkowska A, Goryń T, Pieńkowski A, Wągrodzki M, Jagiełło-Wieczorek E, Rogala P, et al. Denosumab treatment of inoperable or locally advanced giant cell tumor of bone. Oncol Lett. 2016;12(6):4312-8.
111. Gossai N, Hilgers MV, Polgreen LE, Greengard EG. Critical hypercalcemia following discontinuation of denosumab therapy for metastatic giant cell tumor of bone. Pediatr Blood Cancer. 2015;62(6):1078-80.
112. Herr I, Sähr H, Zhao Z, Yin L, Omlor G, Lehner B, et al. MiR-127 and miR-376a act as tumor suppressors by in vivo targeting of COA1 and PDIA6 in giant cell tumor of bone. Cancer Lett. 2017;409:49-55.
113. Forsyth RG, De Boeck G, Baelde JJ, Taminiau AH, Uyttendaele D, Roels H, et al. CD33+ CD14- phenotype is characteristic of multinuclear osteoclast-like cells in giant cell tumor of bone. J Bone Miner Res. 2009;24(1):70-7.
114. Kajihara M, Sugawara Y, Sakayama K, Kikuchi K, Mochizuki T, Murase K. Evaluation of tumor blood flow in musculoskeletal lesions: dynamic contrast-enhanced MR imaging and its possibility when monitoring the response to preoperative chemotherapy-work in progress. Radiat Med. 2007;25(3):94-105.
115. Aoki J, Watanabe H, Shinozaki T, Takagishi K, Ishijima H, Oya N, et al. FDG PET of primary benign and malignant bone tumors: standardized uptake value in 52 lesions. Radiology. 2001;219(3):774-7.
116. McKinney AM, Reichert P, Short J, Dhurairaj T, SantaCruz K, McKinney Z, et al. Metachronous, multicentric giant cell tumor of the sphenoid bone with histologic, CT, MR imaging, and positron-emission tomography/CT correlation. AJNR Am J Neuroradiol. 2006;27(10):2199-201.
117. Girolami I, Mancini I, Simoni A, Baldi GG, Simi L, Campanacci D, et al. Denosumab treated giant cell tumour of bone: a morphological, immunohistochemical and molecular analysis of a series. J Clin Pathol. 2016;69(3):240-7.

118. Gaston CL, Grimer RJ, Parry M, Stacchiotti S, Dei Tos AP, Gelderblom H, et al. Current status and unanswered questions on the use of Denosumab in giant cell tumor of bone. Clin Sarcoma Res. 2016;6(1):15.
119. Zhang J, Tu Q, Grosschedl R, Kim MS, Griffin T, Drissi H, et al. Roles of SATB2 in osteogenic differentiation and bone regeneration. Tissue Eng Part A. 2011;17(13-14):1767-76.
120. Komori T. Regulation of osteoblast differentiation by transcription factors. J Cell Biochem. 2006;99(5):1233-9.
121. Liu W, Toyosawa S, Furuichi T, Kanatani N, Yoshida C, Liu Y, et al. Overexpression of Cbfa1 in osteoblasts inhibits osteoblast maturation and causes osteopenia with multiple fractures. J Cell Biol. 2001;155(1):157-66.
122. Liu TM, Lee EH. Transcriptional regulatory cascades in Runx2-dependent bone development. Tissue Eng Part B Rev. 2013;19(3):254-63.
123. Min JK, Kim YM, Kim YM, Kim EC, Gho YS, Kang IJ, et al. Vascular endothelial growth factor up-regulates expression of receptor activator of NF-kappa B (RANK) in endothelial cells. Concomitant increase of angiogenic responses to RANK ligand. J Biol Chem. 2003;278(41):39548-57.
124. Min JK, Cho YL, Choi JH, Kim Y, Kim JH, Yu YS, et al. Receptor activator of nuclear factor (NF)-kappaB ligand (RANKL) increases vascular permeability: impaired permeability and angiogenesis in eNOS-deficient mice. Blood. 2007;109(4):1495-502.
125. Mak IW, Evaniew N, Popovic S, Tozer R, Ghert M. A Translational Study of the Neoplastic Cells of Giant Cell Tumor of Bone Following Neoadjuvant Denosumab. J Bone Joint Surg Am. 2014;96(15):e127.
126. Den Dunnen, et.al. HGVS recommendations for the description of sequence variants - 2016 update. Hum Mutat. 2016;37:564 - 9.
127. Tsukamoto S, Mavrogenis AF, Leone G, Righi A, Akahane M, Tanzi P, et al. Denosumab does not decrease the risk of lung metastases from bone giant cell tumour. Int Orthop. 2019;43(2):483-9.

Attachment

Spezielles Forschungsmodul 1.10. – 6.11.

Laborprotokoll: 1.10. – 15.10.2020

Arbeiten im Orthopädielabor unter der Leitung von Priv.-Doz. Dr. Birgit Lohberger, mit Hilfe von MSc Dietmar Glänzer.

1.10., Donnerstag

Basisschulung Zellkulturen:
Wofür braucht man eine Zellkultur? Welche verschiedenen Arten gibt es?

Primärkultur:
aus einem Gewebe entnommen, Mischkultur, welche unterschiedlichste Zellen enthalten kann, nicht immortalisiert → begrenzte Anzahl an Passagen
Zelllinien:
Immortal, genetisch einheitlich
Adhäsionszellen: am Boden einer Flask, 2D oder 3D wachsend
Suspensionszellen: schwimmen frei im Nährmedium (NM) herum, d.h. zentrifugieren vor NM Tausch nötig

Kulturmediumherstellung für SW1353/Cal78

Trypsinierung – Trypanblaufärbung – Zählen mit Neubauerkammer

Flask mit Cal78 Zellen aus Inkubator nehmen → Bench
Absauger ein, NM absaugen
Spülen mit phosphate-buffered saline buffer (PBS; 10 ml), wieder absaugen
5 ml Trypsin auf die Zellen geben, schwenken
5-10 min Inkubation bei 37 Grad, unter dem Mikroskop kontrollieren, wie viele Zellen sich schon gelöst haben
Überführung des Flaskinhalts (abgelöste Zellen im Trypsin, 5 ml) in ein Falkon, 10 ml NM dazu
Zentrifugieren: Gegengewicht 15 ml nicht vergessen, 4 min bei 1300 Umdrehungen
Entfernen des NM-Trypsin Gemisches, vorsichtig absaugen (Zellpellet am Boden nicht mitabsaugen)
<u>Bei SW1353 Zellen</u>: Agglutinationsneigung, dagegen 3 ml Akumax dem Zellpellet hinzufügen und gut vermischen, 5 min in Wärme inkubieren
Verdünnung mit NM (zB 7 ml NM + 3 ml Akumax = 10 ml insg.)
Eprouvette herrichten: 20 µl Trypanblau (färbt abgestorbene Zellen dunkelblau an), 1:1 Zellsuspension (+20 µl Zellen im NM) → Vortex
Neubauerzählkammer anhauchen und Deckglas befestigen, einen kleinen Tropfen aus der Eprouvette in das Zählfeld tropfen

Zählung unter dem Mikroskop:
Jeweils in den zu zählenden Quadraten die Zellzahl ermitteln, Durchschnittswert berechnen, mit einer Konstanten (2 x 10^4) sowie der Verdünnung multiplizieren und mittels Schlussrechnung die gewünschten Zellzahlen berechnen.

BSP: links oben: 68 rechts oben: 65
links unten: 70 rechts unten: 74 → Mittelwert = 69,25
69,25 x 2 x 10^4 x 12 ml (Verdünnungsvolumen) = 1,662 x 10^7 Zellen in 12 ml
→ 1x10^5 in 72 µl
→ 2,5x10^5 in 180 µl
→ 5x10^5 in 361 µl

Chamber Flasks seeden: 2x10^5 (Cal78)

9 Chamber Flasks:

3 je für HE Färbung, IHC Färbung Ki67 und H2AX
3 für unterschiedliche Konzentrationen an Bortezomib
- Kontrolle - 2.5 nM Bortez. - 5 nM Bortez.

Jede Chamber Flask wurde mit 2x10^5 Cal78 Zellen geseedet, in 3 ml NM, Inkubation bei 37 Grad bis Montag

2.10., Freitag

Berechnung der Bortezomib Konzentrationen für 9 Chamber Flasks inkl. Montagsgebrauch:

1 Stock → 10 mM Bortezomib
Endvolumen pro Chamber Flask: 3 ml mit je 0 B., 2.5 nM und 5 nM B.
→ 12 ml jeweils

Erste Verdünnung: 18 µl Nährmedium + 2 µl Bortezomib Stock [10 mM]

Entsprechend einer 1:10 Verdünnung und Herstellung einer 1 mM Bortezomib Lösung

Zweite Verdünnung: 999 µl Nährmedium + 1 µl 1. Verdünnung (1 mM B.)

Entsprechend einer 1:1000 Verdünnung und Herstellung einer 1 µM Bortezomib Lösung in einem Volumen von 1 ml

20 ml = 20,000 µl = gewünschtes Endvolumen.
0 M B. → 20 ml Nährmedium
2.5 nM B. → 20,000 µl: 1000 = 20 µl der 2. Verdünnung (1 µM B.) für 1 nM B.
→ sind 20 x 2.5 = 50 µl für 2.5 nM B. in 20 ml Nährmedium
5 nM → 20 x 5 = 100 µl der 2. Verdünnung für 5 nM B. in 20 ml Nährmedium

WH Selbstständig Trypsinierung – Trypanblaufärbung – Zählen mit Neubauerkammer

Zu ermittelnde Zellzahlen sind heute: 1x10^5, 2.5 x10^5 sowie 5 x10^5 SW1353 Zellen für den Scratch-Versuch. Berechnungen nach obig erläutertem Prinzip.

Seeden der 6well Platte mit SW1353 Zellen

Jeweils 2 Wells mit:
- $1x10^5$ Zellen → entsprechend $1x10^5$ x 12: $1.662 x10^7$ = 72 µl + 3 ml Nährmedium in Zeile A und B Spalte 1
- $2.5x10^5$ Zellen → entsprechend 180 µl + 3 ml Nährmedium in Zeile A und B Spalte 2
- $5x10^5$ Zellen → entsprechend 361 µl + 3 ml Nährmedium in Zeile A und B Spalte 3

Bortezomib Treatment der 9 Chamber Flasks laut Berechnungen

3 Chamber Flasks mit 3 ml reinem NM, 3 mit 3 ml NM + 2.5 nM Bortezomib,
3 mit 3 ml NM + 5 nM Bortezomib

5.10., Montag

6well Platte: Woundhealing Assay

Fotodokumentation der verschiedenen Konfluenzen, Spülen mit PBS, Bortezomib Treatment nach Berechnungen (0 nM Bortezomib/control in Reihe A, 5 nM Bortezomib in Reihe B, je in 3 ml NM)
Scratch mit gelber Pipettenspitze, freihändig

Fotodokumentation der Wells direkt nach dem Treatment.

Fixierung der Chamber Flasks für Färbungen:

Absaugen des NM
Waschen mit PBS
Fixierung in 2-3 ml 4% PFA für 30 min
3x Waschen mit PBS, gefolgt von Lagerung in PBS bei 4 Grad (Kühlschrank)

6.10., Dienstag

24 h Fotodokumentation des Woundhealing Assay:

Scratch nur noch schwierig zu erkennen, kein relevanter Unterschied zwischen Kontroll-Wells und mit 5 nM Bortezomib getreateten Wells erkennbar. Als mögliche Ursachen kommen folgende in Betracht:
- Zu häufiges Auftauen des Bortezomib Stocks könnte die proliferationshemmende Wirkung von Bortezomib beeinträchtigt haben.
- Zu hohe Anzahl an Zellen könnte zur zu schnellen Überwucherung geführt haben.
- Zu geringe Stärke des Strichs/scratch.

Erklärung der Funktion eines Schlittenmikrotoms am Beispiel von Herzgewebeschnitten

HE Färbung der 3 Chamber Flasks mit je 2x10^5 Cal78 Zellen, aber unterschiedlichen Bortezomib Konzentrationen

Herstellung von PBS 1x: 100 ml (10%) PBS 10x von Gibco + 900 ml Aqua dest
Entfernung des NM, Boxen über der Plastikplatte, an welcher die Zellen angewachsen sind, entfernen (Herunterbrechen)
Einlegung in einer Küvette mit Tragerl, 15 min in Xylol
Absteigende Alkoholreihe: 100%, 90%, 70% und 50%iges Alkoholbad
Abbrechen des Versuchs, da sich die Plastikscheibe, auf welcher die Zellen gewachsen sind, durch das Xylol und die absteigende Alkoholreihe aufzulösen beginnt und eine gummiartige zerfließende Konsistenz annimmt

7.10., Mittwoch

IHC Färbung der 3 Chamber Flasks mit je 2x10^5 Cal78 Zellen, aber unterschiedlichen Bortezomib Konzentrationen - H2AX

Wie zu Beginn der HE Färbung die Boxen der ChamberFlasks von der Plastikscheibe trennen und das NM verwerfen
Gesamte Küvette mit Tragerl 2x in PBS waschen
Seifiges PBS TritonX 0,1%: auf die Platten je 200 µl verteilen:
600 µl für 3 slides, 0,1% Verdünnung vom TritonX: + 0,6 µl TritonX, aus größerer Höhe (4 cm) auf die slides tropfen (verteilt sich besser); für 10 min einwirken lassen
Waschen mit PBS
Auftitrierung des **1. Antikörpers**:
MERCK, 05-636, Verdünnung 1:200 in Antibody Diluent (aus dem Kühlschrank; 4 Grad)
wieder je 180 – 200 µl je slide: für 3 slides 600 µl Antibody Diluent + 3 µl MERCK AK vorsichtig auf die slides pipettieren, mit Parafilm abdecken, 1 h Inkubation (bei Raumtemperatur; am besten in einer Schublade, Parafilm dient dazu, das Verdampfen zu verhindern)
3x Waschen mit PBS
Brücken-Antikörper: Dako, 0260
1:100 Verdünnung: Für 3 slides 600 µl Antibody Diluent + 6 µl AK
30 min Inkubation bei Raumtemperatur + Parafilm
Dient dem „Brückenschlag“ zwischen dem aus der Maus gewonnenen 1. AK und dem vom Hasen stammenden Rabbit-ON-Rodent
Polymer Rabbit-ON-Rodent-HRP (3 Tropfen aus größerer Höhe auf slides fallen lassen). Mit Parafilm abdecken, 30 min inkubieren bei Raumtemperatur
3x Waschen mit PBS
3 Tropfen Chromogen (AEC) auf die Zellen geben und 2/3 min inkubieren (unter dem Mikroskop den Farbumschlag beobachten, nicht alles zu rot werden lassen)
Schnitte in PBS geben: stoppt die Reaktion
30 sec Kernfärbung mit Hämalaun nach Mayer in der Küvette mit Tragerl
Unter fließendem Leitungswasser 2 min belassen
Eindeckelung mit Aquatex (IHC; bei der HE Färbung: Entellan) – 2 Punkte auf Deckplatte, Objektträger darauf fallen lassen und gegen das Licht schauend die Luftblasen wegdrücken, trocknen lassen

8.10., Donnerstag

IHC Färbung der 3 Chamber Flasks mit je 2x10^5 Cal78 Zellen, aber unterschiedlichen Bortezomib Konzentrationen - Ki67

Wie zu Beginn der HE Färbung die Boxen der ChamberFlasks von der Plastikscheibe trennen und das NM verwerfen
Gesamte Küvette mit Tragerl 2x in PBS Waschen
Seifiges PBS TritonX 0,1%: auf die Platten je 200 µl verteilen:
600 µl für 3 slides, 0,1% Verdünnung vom TritonX: + 0,6 µl TritonX, aus größerer Höhe (4 cm) auf die slides tropfen (verteilt sich besser); 10 min einwirken lassen
Waschen mit PBS
1. Antikörper: Cell Signaling 12202
1:400 Verdünnung in Antibody Diluent (für 3 slides 600 µl Antibody Diluent + 1,5 µl AK)
circa 200 µl aus größerer Höhe auf jedes slide tropfen lassen, mit Parafilm abdecken, 1 Stunde inkubieren (bei Raumtemperatur in einer Schublade zB)
3x mit PBS waschen
130 µl Polymer Rabbit-ON-Rodent-HRP (3 Tropfen) auf jedes slide geben, mit Parafilm abdecken, 30 min inkubieren
3x waschen mit PBS
130 µl Chromogen (AEC) auf die Zellen geben und unter dem Mikroskop den Farbumschlag beobachten (ca 5 min)
Schnitte in PBS geben – Reaktion wird dadurch gestoppt
30 sec Kernfärbung nach Mayer mit Hämalaun
Unter fließendem Leitungswasser bläuen
Schnitte in Aquatex eindeckeln: 2 Punkte auf Deckplatte, Objektträger darauf fallen lassen und gegen das Licht schauend die Luftblasen wegdrücken, trocknen lassen

Auftauen der SW1353 Zellen aus flüssigem Stickstoff

Nach suboptimalen Ergebnissen beim ersten Migrationsassay /Woundhealing-Assay-Versuch sowie gescheiterter HE Färbung sollen diese 2 Versuche mit einem neuen Zellensatz wiederholt werden. Vorsichtsmaßnahmen im Umgang mit flüssigem N: Handschuhe, Gesichts- und Körperschutz benützen.

Auswahl der richtigen Zellen, Ausstreichen der Nummer im Registrierungsbuch
Cryovial aus der entsprechenden Lade im Flüssigstickstofftank entnehmen
Im 37 Grad warmen Wasserbad bei Raumtemperatur auftauen lassen, bis der Inhalt des Cryovials flüssig wird
Vial in ein Falkon mit 10 ml NM überführen
Entfernung des zelltoxischen DMSO mittels Zentrifugation
(1300 Umdrehungen/min für 4 min)
Absaugen des Überstandes, übriggebliebenes Pellet wieder mit 10 ml NM in Flüssigkeit bringen
10 ml NM in ein Flask überführen, beschriften!
Überführung des Falkoninhalts in das Flask. Nun befinden sich die aufgetauten Zellen in insgesamt 20 ml NM und können anwachsen und sich vermehren.
Inkubation bei 37 Grad, erster Wechsel des NM nach 24 h, weitere nach 2/3 Tagen, je nach Zellzahl und Verbrauch/Verfärbung des NM

12.10., Montag

WH Selbstständige Trypsinierung, Trypanblaufärbung, Zählung mit der Neubauer Zählkammer

Zu ermittelnde Zellzahlen sind heute: 2.5 x10^5 sowie 5 x10^5 SW1353 Zellen für den erneuten Scratch-Versuch und die Chamber Flasks (diesmal aus Glas bestehende). Berechnungen nach obig erläutertem Prinzip.

Seeden der 6well Platten

Im 2. Experiment haben wir uns zur Verwendung 2er 6well Platten entschieden, wobei Platte I mit
5 x10^5 SW1353 Zellen und Platte II mit 2.5 x10^5 SW1353 Zellen geseedet wird, jedes Well erhält 3 ml NM. Inkubation bei 37 Grad für 24 h.

Seeden der Chamber Flasks

3 Chamber Flasks aus Glas werden mit 2.5 x10^5 SW1353 Zellen geseedet und erhalten je 2 ml NM.
Inkubation bei 37 Grad für 24 h.

Berechnungen der Bortezomib Verdünnungen

Berechnungen nach obig erläutertem Prinzip. Für die 6well Platten haben wir uns für Bortezomib Konzentrationen von 5 nM und 20 nM entschieden, für die ChamberFlasks werden die gleichen hohen Konzentrationen herangezogen, um die proliferationshemmende Wirkung von Bortezomib besser darstellen zu können. Lagerung der fertigen Falkons im Kühlschrank bei 4 Grad bis morgen.

13.10., Dienstag

Scratch und Bortezomib Treatment der 6well Platten, Fotodokumentation

Im 2. Experiment haben wir nicht nur mehr Wells (jeweils gleiche Untersuchungsgegebenheiten in 2 Wells), sondern auch höhere Bortezomib Konzentrationen und dickere Striche (blaue Pipettenspitze) verwendet. Somit ergeben sich:

Platte I - 5 x10^5 SW1353 Zellen
Reihe A wie Reihe B behandelt, jedes Well mit einer blauen Pipettenspitze durchzogen
- Spalte 1: 3 ml NM, Kontrolle, kein Bortezomib
- Spalte 2: 3 ml NM inklusive 5 nM Bortezomib
- Spalte 3: 3 ml NM inklusive 20 nM Bortezomib

Platte II - 2.5 x10^5 SW1353 Zellen
Reihe A wie Reihe B behandelt, jedes Well mit einer blauen Pipettenspitze durchzogen
- Spalte 1: 3 ml NM, Kontrolle, kein Bortezomib
- Spalte 2: 3 ml NM inklusive 5 nM Bortezomib
- Spalte 3: 3 ml NM inklusive 20 nM Bortezomib

Erneute Inkubation bei 37 Grad.
Eine Fotodokumentation fand 2 h und 6 h nach dem Treatment statt.

Bortezomib Treatment der Chamber Flasks

Absaugen des NM, ein ChamberFlask bleibt als Kontrolle Bortezomib-frei und erhält nur 2 ml NM, eines erhält 2 ml NM inklusive 5 nM Bortezomib und das letzte 2 ml NM inklusive 20 nM Bortezomib. Inkubation erneut bei 37 Grad.

14.10., Mittwoch

24 h Fotodokumentation der 6well Platten

Ohne NM-Wechsel und damit ohne Veränderung der Bortezomibkonzentrationen findet erneut eine Fotodokumentation nach 24 h statt.

Fixation der Chamber Flask Schnitte in 4% PFA

Absaugen des NM
Waschen mit PBS
Fixierung in 2-3 ml 4% PFA für 30 min
3x Waschen mit PBS, gefolgt von Lagerung in PBS bei 4 Grad (Kühlschrank)

15.10., Donnerstag

HE Färbung der 3 Chamber Flasks

Entfernung des NM sowie Herunterbrechen der Boxen über der Glasplatte, an welcher die Zellen angewachsen sind
Einlegung in einer Küvette mit Tragerl, 15 min in Xylol
Absteigende Alkoholreihe: 100%, 90%, 70% und 50%iges Alkoholbad
Kurz in Aqua dest. stellen
3 min lang Kernfärbung in Hämalaun nach Mayer
4 min unter fließendem Leitungswasser bläuen
1,5 min lang in Eosin färben
Aufsteigende Alkoholreihe: zuerst 90%, dann 100% Ethanol
In Butylacetat stellen (=Lösungsmittel für das Eindeckmittel, da es sich um eine HE Färbung handelt: Entellan)
Eindeckeln mit Entellan: recht großzügige Tropfen auf ein Deckglas tropfen und die Schnitte wieder darauf fallen lassen. Gegen das Licht schauend die Luftblasen wegdrücken.
Trocknen lassen

Fotodokumentation aller HE, IHC H2AX und Ki67 Färbungen

Verschiedene Größen wurden hierbei verwendet: 60x und 40x für die IHC Färbungen, 10x für die HE Färbungen.

48 h Fotodokumentation der 6well Platten

Nach diesmal geglücktem Experiment werden die 6well Platten verworfen.

Woundhealingassay, 2. Versuch 5 x10^5 SW1353 Zellen, 10x Vergrößerung

Nach 2 h Nach 24 h Nach 48 h

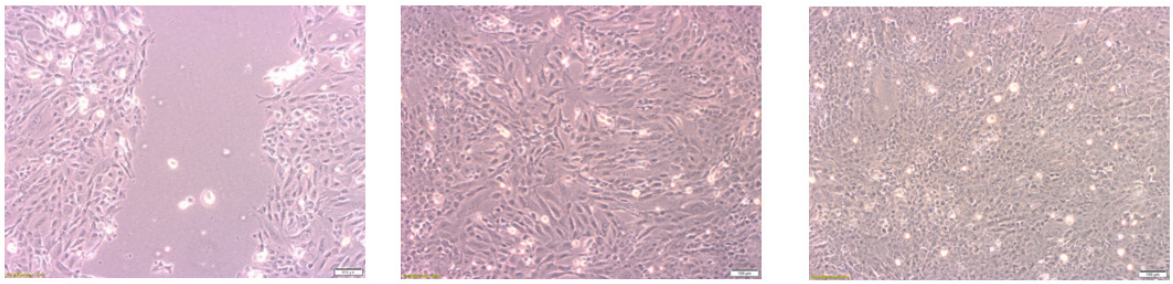

→ Ohne Bortezomib

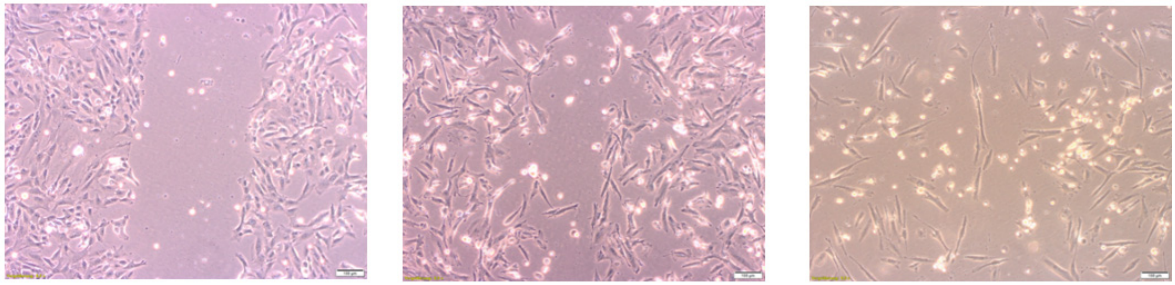

→ Mit 20 nM Bortezomib

Die wachstumshemmende Wirkung von Bortezomib in der unteren Bildreihe ist deutlich erkennbar, auch wenn die Grenzen des mittels einer blauen Pipettenspitze gezogenen Strichs mit der Zeit verschwinden.

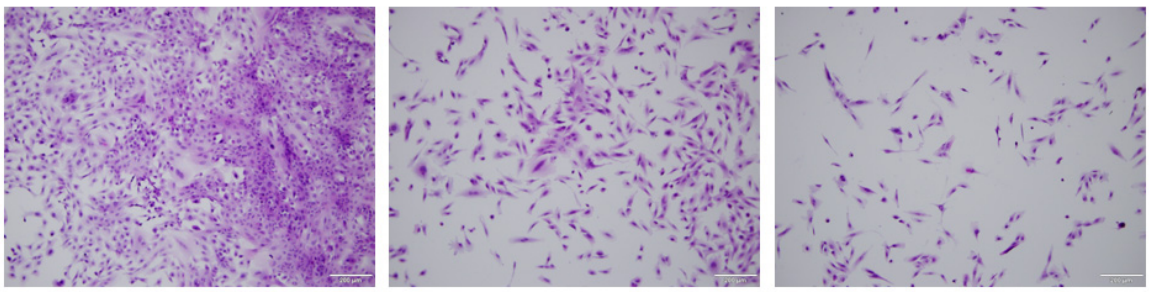

2,5 x10^5 SW1353 Zellen, 10x Vergrößerung, Kontrolle

2,5 x10^5 SW1353 Zellen, 10x Vergrößerung, **5** nM Bortezomib

2,5 x10^5 SW1353 Zellen, 10x Vergrößerung, **20** nM Bortezomib

→ **Hämatoxylin-Eosin Färbung**

Auch die HE Färbung zeigt deutlich vermindertes Zellwachstum bei 20 nM Bortezomib.

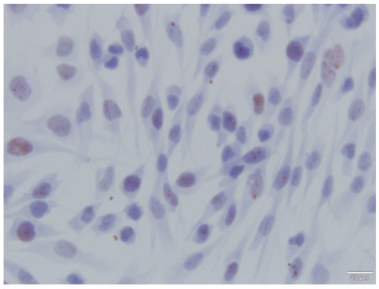

2 x10^5 Cal78 Zellen,
60x Vergrößerung,
Kontrolle

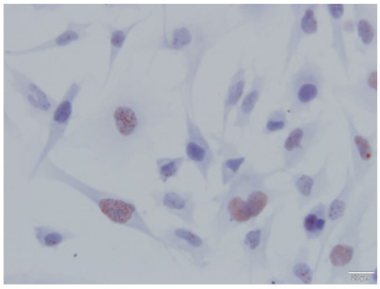

2 x10^5 Cal78 Zellen,
60x Vergrößerung,
2,5 nM Bortezomib

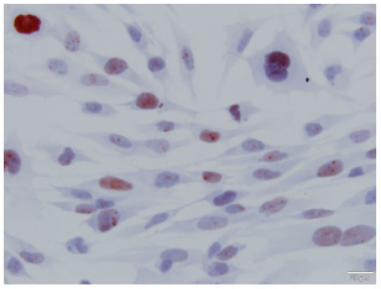

2 x10^5 Cal78 Zellen,
60x Vergrößerung,
5 nM Bortezomib

→ H2AX, Immunhistochemische Färbung

H2AX ist ein Marker für DNA Schäden, je roter sich die Zellen also anfärben, desto mehr DNA Schäden sind in diesen Zellen zu finden. In der Kontrollgruppe findet sich demnach kaum bis wenig Schädigung, wohingegen sich in den mit 5 nM Bortezomib behandelten Zellen deutlich mehr Schädigung zeigt.

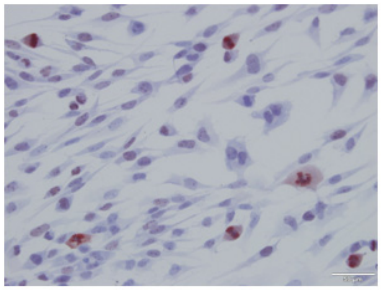

2 x10^5 Cal78 Zellen,
40x Vergrößerung,
Kontrolle

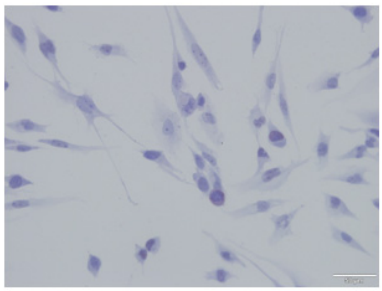

2 x10^5 Cal78 Zellen,
40x Vergrößerung,
2,5 nM Bortezomib

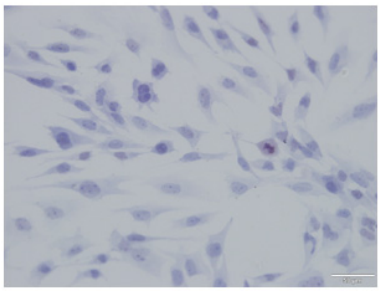

2 x10^5 Cal78 Zellen,
40x Vergrößerung,
5 nM Bortezomib

→ Ki67, Immunhistochemische Färbung

Ki67 ist ein weithin verbreiteter und häufig angewendeter Marker für Proliferation. In dem Bild, welches Zellen der Kontrollgruppe (ohne Bortezomib) zeigt, findet sich im rechten unteren Viertel des Bildes sogar eine Zelle, die sich gerade teilt und demnach rot angefärbt ist. In den mit Bortezomib behandelten Zellen dagegen findet sich sehr wenig rot angefärbtes Material, entsprechend einer stark ausgeprägten Proliferationshemmung, vermittelt durch Bortezomib.